



Recent advances in non-noble metal-based bifunctional electrocatalysts for overall seawater splitting



Hao Zhang^{a,b,1}, Yang Luo^{c,d,1}, Paul K. Chu^c, Qian Liu^e, Xijun Liu^{f,*}, Shusheng Zhang^g, Jun Luo^b, Xinzhong Wang^{a,*}, Guangzhi Hu^{h,i,**}

^a Information Technology Research Institute, Shenzhen Institute of Information Technology, Shenzhen 518172, China

^b Institute for New Energy Materials & Low-Carbon Technologies and Tianjin Key Lab of Photoelectric Materials & Devices, School of Materials Science and Engineering, Tianjin University of Technology, Tianjin 300384, China

^c Department of Physics, Department of Materials Science and Engineering, and Department of Biomedical Engineering, City University of Hong Kong, Tat Chee Avenue, Kowloon, Hong Kong, China

^d Empa, Swiss Federal Laboratories for Materials Science and Technology, ETH Domain, Dübendorf 8600, Switzerland

^e Institute for Advanced Study, Chengdu University, Chengdu 610106, Sichuan, China

^f MOE Key Laboratory of New Processing Technology for Non-Ferrous Metals and Materials, and Guangxi Key Laboratory of Processing for Non-Ferrous Metals and Featured Materials, School of Resource, Environments, and Materials, Guangxi University, Nanning 530004, China

^g College of Chemistry, Zhengzhou University, Zhengzhou 450000, China

^h Institute for Ecological Research and Pollution Control of Plateau Lakes, School of Ecology and Environmental Science Yunnan University, Kunming 650091, China

ⁱ Department of Physics, Umeå University, Umeå 901 87, Sweden

ARTICLE INFO

Article history:

Received 12 May 2022

Received in revised form 20 June 2022

Accepted 30 June 2022

Available online 6 July 2022

Keywords:

Non-noble metals

Bifunctional electrocatalysis

Water splitting

Seawater

ABSTRACT

Since seawater is one of the most abundant resources on earth, seawater electrolysis is becoming increasingly attractive for clean energy/hydrogen production. Although significant progress has been made recently, it is still challenging to obtain bifunctional electrocatalysts with high catalytic activity and durability suitable for seawater electrolysis because of the scarcity of precious metals and inadequate state-of-the-art materials for the overall reaction. The development of high-performance bifunctional electrocatalysts is crucial to the commercialization of overall seawater electrolysis and in this review, the mechanism and challenges of seawater electrolysis are introduced. Optimization strategies for different types of non-noble-metal-based electrocatalysts including structural regulation, interface regulation, doping regulation, *in situ* assembly, alloying, and amorphization are summarized to elucidate the relationship among composition, structure, and properties. Finally, the challenge and prospective for future development of non-noble-metal-based bifunctional catalysts are discussed. This paper aims at providing guidance and insights into the rational design of highly efficient catalytic materials for practical seawater splitting.

© 2022 The Author(s). Published by Elsevier B.V.
CC_BY_4.0

Contents

1. Introduction	2
2. Challenges of overall seawater electrolysis	2
2.1. Challenges in HER	3
2.2. Challenges in OER	3
3. Strategies for design and optimization of electrocatalysts	3
3.1. Structural regulation	3

* Corresponding authors.

** Corresponding author at: Institute for Ecological Research and Pollution Control of Plateau Lakes, School of Ecology and Environmental Science Yunnan University, Kunming 650091, China.

E-mail addresses: xjliu@tjut.edu.cn (X. Liu), wangxz@sziit.com.cn (X. Wang), guangzhi.hu@umu.se (G. Hu).

¹ These authors contributed equally to this work.

3.2. Interface regulation	4
3.3. Doping regulation	6
3.3.1. Single-element doping	7
3.3.2. Dual-element doping	9
3.4. Others	9
4. Summary and outlook	12
Data Availability	12
Declaration of Competing Interest	13
Acknowledgements	13
References	13

1. Introduction

Extensive use of fossil fuels has exacerbated environmental pollution due to the emission of a large amount of carbon dioxide (CO_2) which may cause the greenhouse effect [1] and more countries are committing to the transition to clean and green energy to achieve carbon neutrality [2]. Hydrogen (H_2) is a clean, sustainable, carbon-free energy source with high specific energy compatibility and a desirable candidate to replace fossil fuels [3,4]. At present, more than 96% of the world's H_2 still comes from the reformation of fossil fuels and this process itself emits a large amount of CO_2 . Hence, an attractive alternative is to produce hydrogen and oxygen by water splitting using thermal, photocatalytic or electrocatalytic techniques and in particular, electrocatalytic water electrolysis is a hot research topic.

Water electrolysis consists of two half reactions, the oxygen evolution reaction (OER) at the anode and hydrogen evolution reaction (HER) at the cathode. Both reactions require highly efficient electrocatalysts to offset the slow kinetics and achieve high energy efficiency. In the electrolytic cell system, the theoretical voltage required to achieve overall water splitting is 1.23 V. However, in the actual commercial seawater splitting system, a voltage of 1.8–2.0 V is required to drive water splitting to generate clean energy H_2 . In order to reduce the HER and OER overpotentials and accelerate the reactions, high-efficiency bifunctional catalysts are imperative. As shown in Fig. 1, the hydrogen adsorption free energy (ΔG_{H}) directly reflects the hydrogen evolution efficiency, and its absolute value close to 0 means that the corresponding catalyst shows better activity, so Pt-based metals have better HER activity than other metals [5]. Similarly, the free energy difference of intermediate formation ($\Delta G_{\text{O}} - \Delta G_{\text{OH}}$) reflects the oxygen evolution efficiency, and its

absolute value close to 1.6 means that the corresponding catalysts act as more competitive candidates, so noble metal oxides such as IrO_2 and RuO_2 have excellent OER activity [6]. But the high price, natural scarcity, and poor stability of precious metals hinder the practical development of new energy conversion and storage technologies.

Non-noble metal-based catalysts, such as transition metal and its heterozygous structure catalysts such as carbon-based catalysts, etc., have become one of the most attractive substitutes for noble metal catalysts due to their high catalytic activity, excellent stability and low price in HER or OER. Nevertheless, there are very few bifunctional non-noble metal-based catalysts that meet the requirements for overall seawater hydrolysis. Therefore, it is urgent to develop non-noble-metal-based electrocatalysts with high activity and stability and in recent years, non-noble-metal electrocatalysts with modulated electronic structure, high conductivity, and optimized adsorption energy of the intermediates have been actively explored [7].

This review describes the mechanism of electrocatalytic water splitting and challenges encountered by commercial seawater electrolysis. Effective strategies to improve the selectivity and stability of bifunctional electrocatalysts are presented and challenges and prospective of seawater electrolysis are discussed.

2. Challenges of overall seawater electrolysis

The electrolysis of natural seawater is similar to pure water and is divided into two half-reactions, HER at the cathode and OER at the anode. However, seawater electrolysis is more complicated due to the existence of many side reactions.

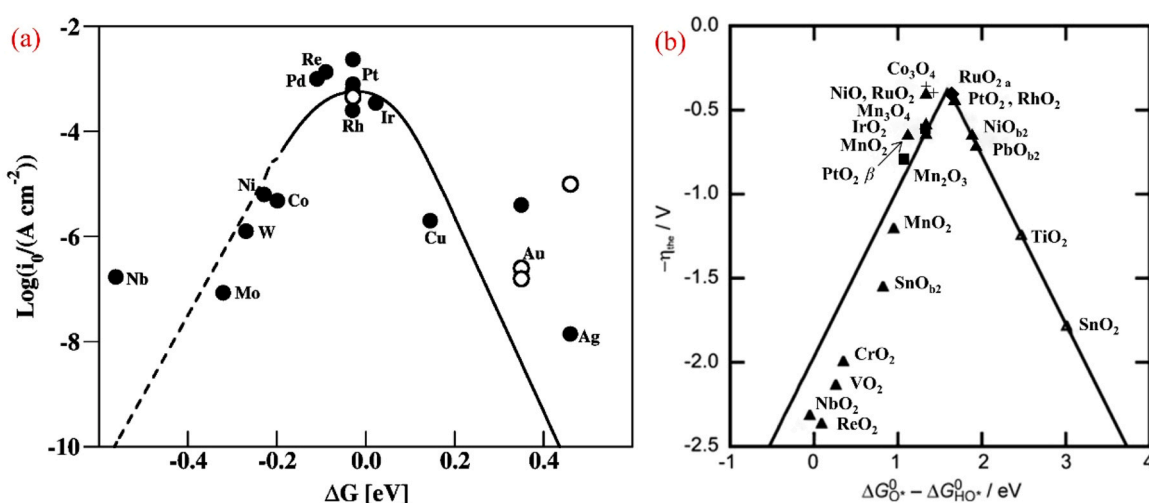
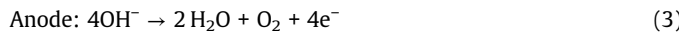
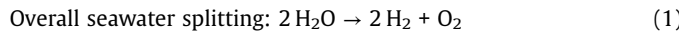


Fig. 1. (a) The relationship between i_0 and ΔG_{H} for various metals on HER volcano plot. (b) The relationship between $\eta̅$ and $\Delta G_{\text{O}}^0 - \Delta G_{\text{OH}}^0$ for various metal oxides on the OER volcano plot.

(a) Reproduced with permission from ref. [5]. Copyright (2010), American Chemical Society. (b) Reproduced with permission from ref. [6]. Copyright (2011), Wiley-VCH.

Table 1
Chemical composition of seawater [10–13].

Elements	Concentration (ppm)	Chemical species
Cl	~19500–22014	Cl ⁻
Na	~11536–14039	Na ⁺
Mg	~1290–1543	Mg ²⁺
S	~905–3273	SO ₄ ²⁻ , NaSO ₄ ⁺
Ca	~378–420	Ca ²⁺
K	~380–470	K ⁺
Br	~67	Br ⁻
C	~28	HCO ₃ ⁻ , CO ₃ ²⁻
N	~12	NO ₃ ⁻ , NH ₄ ⁺



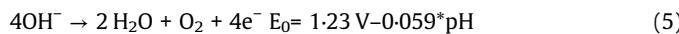
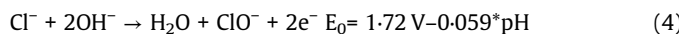
At present, seawater electrolysis shows great promise in future hydrogen production, but the industrial application still has a long way to go because of some stoppers to be discussed in this section.

2.1. Challenges in HER

The energy barrier for HER is higher in neutral seawater compared to the acidic electrolytes rich in H⁺, which leads to slow HER kinetics. For HER with the increase of electrolysis current, the local pH value near the cathode increases, resulting in the precipitation of various dissolved ions (Table 1) in seawater and covering the surface of the active site, thereby reducing the active center of the cathode. In addition, bacteria and microbes may corrode and poison the electrodes, seriously affecting their stability in seawater [8,9].

2.2. Challenges in OER

In addition to the effects of bacteria and microorganisms mentioned above, the fact that OER is a four-electron process and involves multiple intermediates results in inherently poor kinetics and thus requires higher overpotentials to drive. Another major challenge of seawater electrolysis is chlorine evolution reaction (CER), which typically occurs at the anode and competes with OER at a relatively high overpotential and chloride ions corrode the electrodes [14,15]. Dresp et al. [16] have listed the possible redox reactions during seawater electrolysis. NaCl and KCl produce CER at the anode and compete with OER on the anode against H₂/O₂ production at overpotentials well below ClO⁻ formation according to the following Eqs. (4) and (5):



Eqs. (1) and (2) indicate that CER involves only two electrons, which may have faster dynamics than the four-electron transfer OER. However, the Pourbaix diagram (Fig. 2) shows that OER has a higher thermodynamic redox potential than the CER at all pH values [17]. In the alkaline system (blue region in Fig. 2), a standard potential of CER is 480 mV higher than that of OER, but the difference is smaller in the acidic environment. Therefore, OER is required to be kept at a low overpotential of less than 480 mV to produce O₂ and to prevent chlorine precipitation in the alkaline medium.

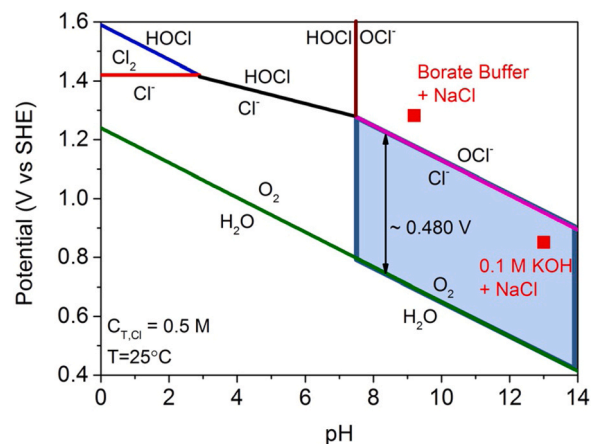


Fig. 2. Pourbaix diagram of simulated seawater (0.5 M NaCl solution) representing the oxygen and chlorine systems.
Reproduced with permission from ref. [18]. Copyright(2016), Wiley-VCH

3. Strategies for design and optimization of electrocatalysts

3.1. Structural regulation

It is well known that the current densities of catalysts increase with the active center densities and more active centers translate into higher electrocatalytic activity. Structural modulation is a promising way to enhance the density of active sites [19–37] and the optimized structures also play a key role in mitigating electrode corrosion in seawater. Seawater electrocatalysts with the sandwiched structure, core-shell structure, nanorods, and nanosheets have been proposed for overall seawater splitting (Table 2). By designing the proper surface morphology, a large specific surface area and high surface activity can be achieved and the contact area between the electrode and electrolyte (seawater) can be improved to facilitate the transfer of electrons, ions, and reaction products.

Wood with a unique anisotropic multi-channelled structure is economical and widely available. Chen et al. [38] have removed hemicellulose and lignin from natural balsa wood and coated the NiMoP alloy (loading: 12.87 mg cm⁻²) on wood aerogel to produce the sandwiched S, P-(Ni, Mo, Fe)OOH/NiMoP/wood aerogel electrocatalyst by a one-step method (Fig. 3a). Owing to the open and aligned micro-channels (Fig. 3d), large specific surface area, good wetting ability of 3D wood aerogel, as well as high conductivity, adhesion strength, and corrosion resistance of NiMoP (Fig. 3e), the assembled electrolyzer with S, P-(Ni, Mo, Fe)OOH/NiMoP/wood aerogel as the two electrodes, shows efficient and stable catalytic characteristics such as a current density of 500 mA cm⁻² at 1.861 V in 1 M KOH seawater and robust cycling.

Utilizing the anticorrosion performance of Ni_x in seawater, Li et al. [39] have developed a Ni₃S₂-1T-MoS₂-Ni₃S₂ (NMN) multi-layered coat on the Ni substrate by a two-step hydrothermal process (Fig. 3f). The water-splitting cell with NMN-NF as both anode and cathode requires a voltage of 1.82 V for a current density of 100 mA/cm⁻² and stable overall water splitting can be performed in 1 M KOH seawater for 100 h at 100 mA/cm⁻². The top Ni₃S₂ layer (a1 area) consisting of large and aggregated nanoparticles in the NMN-NF sandwiched structure (Fig. 3g) is mainly responsible for the HER process, while the bottom one (a3 area) for the OER due to the electron deficiency in the Ni oxidation state. The MoS₂ interlayer (a2 area) with microspheres boosts the HER and OER performance. The Ni₃S₂ layer in the unique sandwiched structure serves as a shield to provide the corrosion resistance against chloride anions to enhance the long-term durability. In addition, NMN-NF has other advantages

Table 2

Comparison of recently reported electrocatalysts for overall seawater splitting pertaining to structural regulation.

Electrodes	Voltage (V) @ current density (mA cm^{-2})	Durability (h)	Electrolytes	Refs.
S,P-(Ni,Mo,Fe)OOH /NiMoP/wood aerogel	1.861 @ 500	10	1 M KOH + seawater	[36]
NMN-NF	1.82 @ 100	100	1 M KOH + seawater	[37]
GO@Fe@Ni-Co@NF	2.02 @ 1000	378	1 M KOH + 0.5 M NaCl	[38]
S-NiMoO ₄ @NiFe-LDH	1.68 @ 100	20	1 M KOH + 0.5 M NaCl	[39]
	1.73 @ 100	20	1 M KOH + seawater	
Au-Gd-Co ₂ B @TiO ₂	1.74 @ 1000	200	1 M KOH + seawater	[41]

such as the large surface area, large density of active sites, and small charge transfer resistance in overall seawater splitting.

The core-shell structure improves the stability of seawater electrolysis. Jadhav et al. [40] have synthesized the FeOOH deposited β -Ni-Co hydroxide supported on nickel foam catalyst (GO@Fe@Ni-Co@NF) catalyst (loading: 1.9 mg cm^{-2}) with an outer graphene oxide layer by a three-step hydrothermal-annealing-electrodeposition process (Fig. 4a). The charge transfer resistance is lower and corrosion resistance is improved by the metal oxide layer underneath, β -Ni-Co LDH with a small interlayer distance, GO overlayer, and oxidized carbon layer generated *in situ*. To accomplish current densities of 20 mA cm^{-2} and 1000 mA cm^{-2} in $1 \text{ M KOH} + 0.5 \text{ M NaCl}$ at room temperature, the as-prepared electrolyzer with GO@Fe@Ni-Co@NF acted as both the anode and cathode, only requires very low voltages of 1.57 and 2.02 V, respectively and remarkable stability is demonstrated for 378 h at a current density of 1000 mA cm^{-2} .

Wang et al. [41] have synthesized a 3D core-shell electrocatalyst with the NiFe-LDH layer anchored on S-NiMoO₄ nanorods supported by the porous Ni foam (S-NiMoO₄ @NiFe-LDH) by the three-step hydrothermal-vulcanization-electrodeposition technique (Fig. 4b) and the catalyst offers abundant active sites, rapid electron transfer, and good corrosion resistance. The NiFe-LDH layer plays the primary role in OER and the S-NiMoO₄ nanorods beneath are responsible for HER in the simulated alkaline seawater electrolyte. A current density of 100 mA cm^{-2} is achieved by applying voltages of 1.68 and 1.73 V,

and the voltages are lower than those of the $\text{IrO}_2 \parallel \text{Pt/C}$ pair (1.73 and 1.81 V, respectively) in simulated and natural alkaline seawater [42].

In addition to 3D structures on self-supporting materials, 2D structures have been constructed. Haq et al. [43] have proposed a strategy to assemble Au nanocluster decorated Gd-Co₂B nanoflakes embedded in TiO₂ nanosheets on the Ti foil (Au-Gd-Co₂B@TiO₂) (loading: 0.2 mg cm^{-2}) for seawater electrolysis. Benefiting from the large surface area, abundant active sites, high conductivity, and excellent corrosion resistance, the electrolyzer with Au-Gd-Co₂B@TiO₂ working as both the anode and cathode electrodes needs a low voltage of 1.74 V to attain a current density of 1000 mA cm^{-2} with no significant decline for over 200 h in 1 M KOH seawater.

3.2. Interface regulation

With regard to heterogeneous catalysts, it is essential to design the appropriate interface to increase the active sites [44] and promote charge transfer between the electrocatalyst and electrolyte at the interface. This can be accomplished by interfacial modulation [45–56] and a series of heterostructures have been prepared to enhance the overall seawater splitting characteristics (Table 3).

Owing to their high electrical conductivity, Nitride- and sulfide-based compounds are considered promising water splitting electrocatalysts [57,58]. However, the lack of active sites greatly hinders

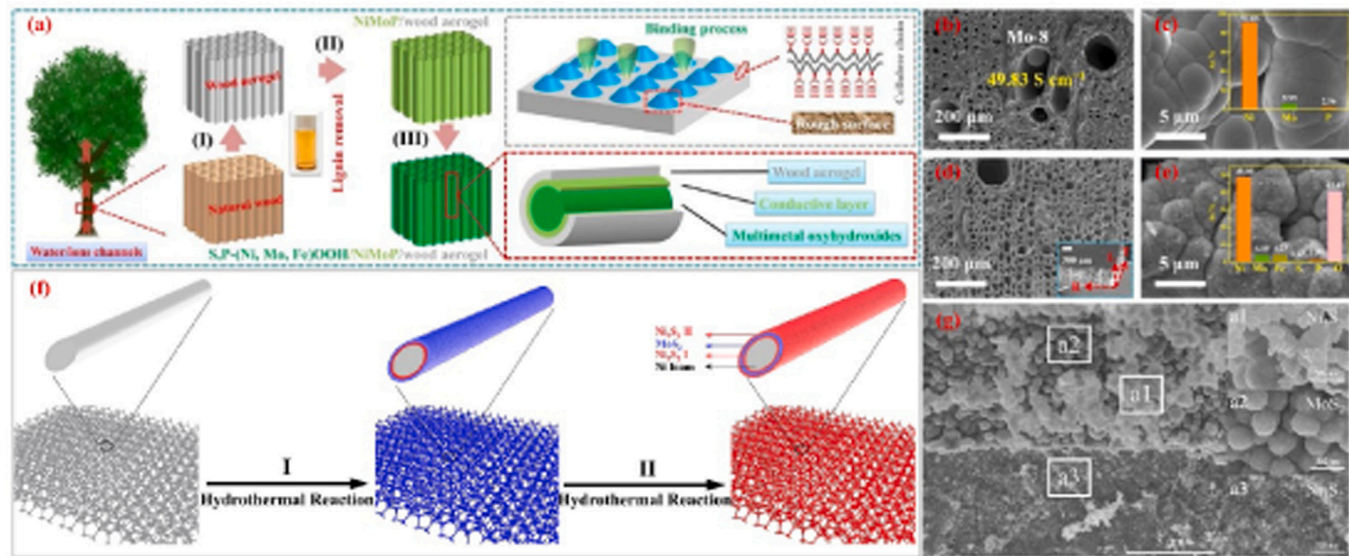


Fig. 3. (a) Schematic illustration of the synthesis procedure for the S, P-(Ni, Mo, Fe)OOH/NiMoP/wood aerogel electrocatalyst with corresponding steps. (I) Removal of hemi-cellulose and lignin, (II) Preparation of NiMoP alloys coated on the wood aerogel, and (III) Surface construction of S, P-(Ni,Mo,Fe)OOH on the NiMoP alloys/wood aerogel. SEM images of the NiMoP/wood aerogel (b, c) and S and P-(Ni,Mo,Fe)OOH/NiMoP/wood aerogel. (f) Schematic diagram of the formation process of NMN-NF. (g) SEM images of NMN-NF with various magnifications.

(d, e). Reproduced with permission from ref. [38]. Copyright (2021), Elsevier. (g) Reproduced with permission from ref. [39]. Copyright (2021), Elsevier.

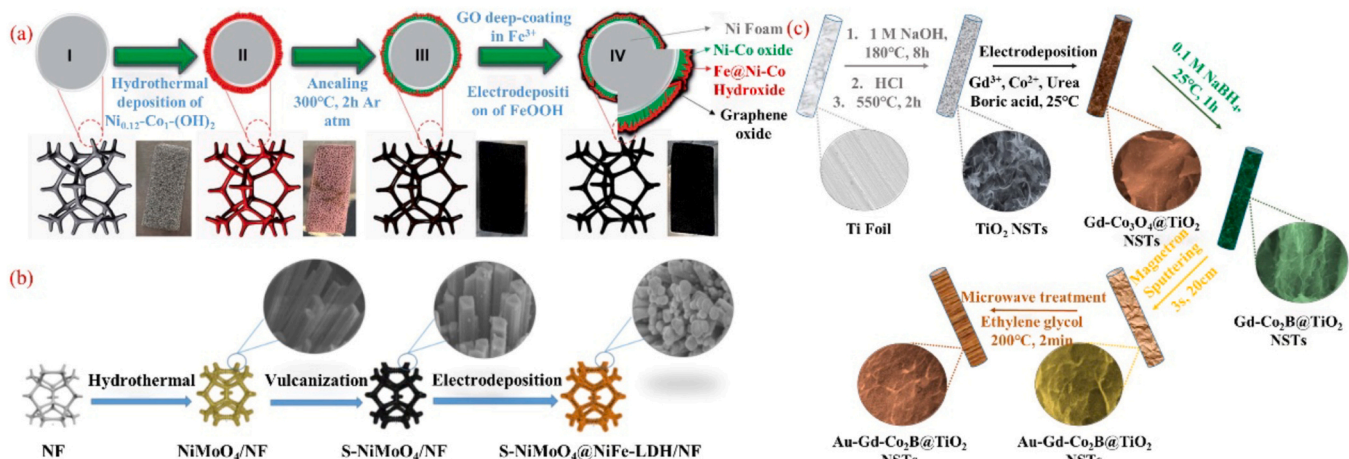


Fig. 4. (a) Schematic illustrating the fabrication processes for the free-standing GO@Fe@Ni-Co@NF electrode and corresponding intermediates steps [II: Ni-Co hydroxide@NF, III: Ni-Co@NF, IV: GO@Fe@Ni-Co@NF]. (b) Schematic illustration for the synthesis of the S-NiMoO₄@NiFe-LDH NS core-shell structure. (c) Systematic illustration of the preparation of Au-Gd-Co₂B@TiO₂.

(a) Reproduced with permission from ref. [40]. Copyright (2020), Royal Society of Chemistry. (b) Reproduced with permission from ref. [39]. Copyright (2022), Elsevier. (c) Reproduced with permission from ref. [41]. Copyright (2022), Elsevier.

Table 3

Comparison of recently reported electrocatalysts for overall seawater splitting pertaining to interface regulation.

Electrodes	Voltage (V) @ current density (mA cm ⁻²)	Durability (h)	Electrolytes	Refs.
NiNS	1.8 @ 48.3	–	seawater	[55]
cRu-Ni ₃ N/NF	1.62 @ 50	–	1 M KOH + seawater	[56]
	1.73 @ 100			
Ni ₂ P-Fe ₂ P/NF	1.811 @ 100	38	1 M KOH + seawater	[65]
	2.004 @ 500	48		
NiCo ₂ S ₄ /NiMo ₂ S ₄ /NiO	1.505 @ 100	720	5 M KOH + seawater, 80 °C	[66]

the improvement of their electrocatalytic activities. It has been shown that the interface plays a significant role in accelerating dissociative adsorption of water [59] and improving the kinetics in electrochemical water electrolysis [60]. Zhao et al. [61] have fabricated a nickel nitride/sulfide (NiNS) electrode with abundant interfacial contact by simple one-step calcination of nickel foam with thiourea in a vacuum-sealed ampoule. The interface between the various planes of Ni_3N (loading: 9.27 mg cm⁻²) and Ni_3S_2 (loading: 10.68 mg cm⁻²) species in polycrystalline NiNS (Fig. 5a) is observed by HR-TEM (Fig. 5b and c) and serves as electrocatalytic active sites for dissociative adsorption of water molecules and subsequent water electrolysis. The two-electrode electrolyzer with NiNS // NiNS couple shows a current density of 48.3 mA cm⁻² at 1.8 V higher than that of the Ir-C // Pt-C (2.9 mA cm⁻²) in seawater. Through the study of electrochemical active sites, the electrocatalytic mechanism was explored, which suggested that the abundant interfacial regions predominantly accounted for the excellent catalytic performance.

Ni_3N has been adopted to build a strong coupling interface with Ru. Zhu et al. [62] have observed that Ru has a terrific lattice similar to Ni_3N and the unusual epitaxial hetero-interface can be obtained by exploiting the similar lattices in the two different materials [63,64]. They have assembled cRu-Ni₃N porous nanosheets on the conductive nickel foam to form cRu-Ni₃N/NF (Fig. 5d). During nitridation, the tiny Ru clusters are grown epitaxially *in situ* on the Ni₃N nanosheets to form strongly coupled heterointerfaces (Fig. 5e) at which the charge density is redistributed and the electron-enriched hetero-interfaces improve the intrinsic electron conduction. Consequently, adsorption of the key intermediates is modulated,

which changes the rate-determining step and reduces the activation energy barrier in HER and OER (Fig. 5f-i) [65]. The assembled electrolyzer with cRu-Ni₃N/NF acted as both the anode and cathode, delivering excellent catalytic performance (1.62 and 1.73 V @ 50 and 100 mA cm⁻²) with few side reactions, higher selectivity, and good durability in overall seawater splitting, which is superior to the Pt/C || RuO₂ couple (1.70 and 1.84 V). This bifunctional electrode can be directly connected to commercial solar panels (Fig. 5j) and suggests the possibility of large-scale application with other external power supplies.

Heterogeneous bimetallic phosphides have become a hot research topic due to their structural and chemical advantages, for example, ($\text{Ni}_{0.33}\text{Fe}_{0.67}$)₂P [68], FeP/Ni₂P [69], $\text{Ni}_2\text{P}-\text{Cu}_3\text{P}$ [70], Fe-Co-P [71], and NiCoP [72], etc. Wu et al. [66] have synthesized a heterogeneous electrocatalyst with $\text{Ni}_2\text{P}-\text{Fe}_2\text{P}$ micro-sheets supported on Ni foam ($\text{Ni}_2\text{P}-\text{Fe}_2\text{P}/\text{NF}$) (loading: 15.0 mg cm⁻²) by soaking and phosphating. The modification of Fe cations resulted in the formation of rough topography of some nanoparticles on the surfaces of the micro sheets (Fig. 6a) which increase the specific surface area on the electrocatalyst. The hetero-interfaces between the phase boundary of Ni_2P and Fe_2P phases (Fig. 6c) produce the interfacial bonding effect, which is beneficial to exposing more active sites. Owing to the high intrinsic activity, plentiful active sites, an exceptional transfer coefficient, enhanced corrosion resistance, and hydrophilic surface, the as-prepared electrolyzer with $\text{Ni}_2\text{P}-\text{Fe}_2\text{P}/\text{NF}$ as the two electrodes shows excellent catalytic activity and robust durability in overall seawater splitting requiring low voltages of 1.811 and 2.004 V to attain current densities of 100 and 500 mA cm⁻² in 1 M KOH seawater, respectively.

Seenivasan et al. [67] have constructed a heterogeneous multiple transition metal sulfide NCMS/NiO (NCMS/NiO) electrocatalyst by ion exchange with a layer of NiO on the catalyst surface by atomic layer deposition (ALD) to increase the active sites (Fig. 6d). The hollow cuboid NCMS/NiO electrocatalyst shows an obvious hetero-interface between NiCo₂S₄ and NiMo₂S₄ with close contact in the cuboid wall and NiO shell layer over the wall (Fig. 6e-g). An *in situ* reconstruction, occurring on the NiO and the metal sulfide (M-S), led to dual active sites of M-S and metal-oxyhydroxide (M-OOH) (Fig. 6h-j) with good corrosion resistance to chloride ions during high-temperature seawater electrolysis. The thicker NiOOH/NiO layer restricts the diffusion of the electrolyte to the NCMS core thus decreasing the number of active sites and OER activity. The NiO layer with a thickness of 0.2 nm and about the size of a NiO molecule

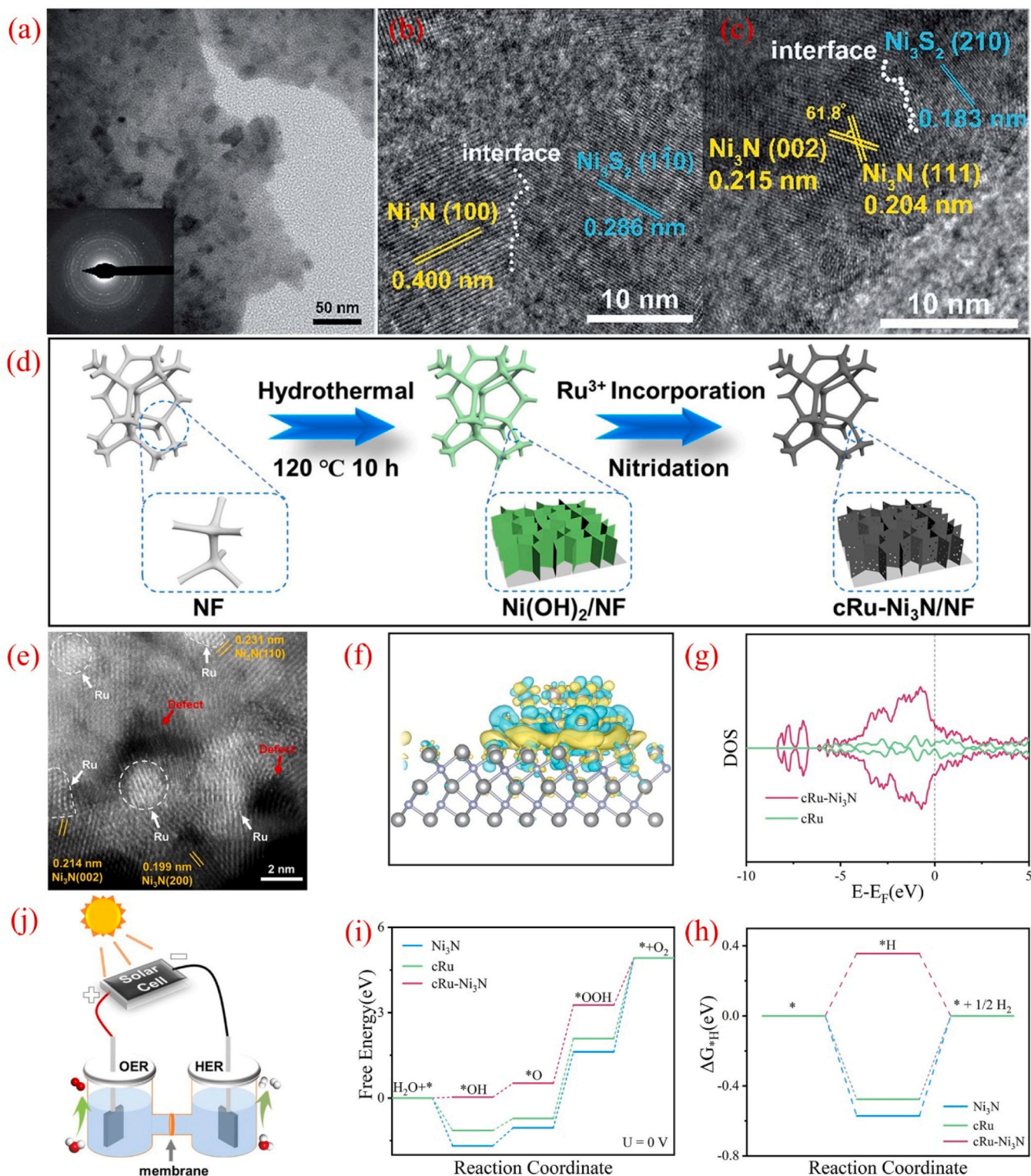


Fig. 5. (a) TEM image and SAED pattern (inset), (b, c) HR-TEM images of NiNS. (d) Schematic illustration of the synthesis for epitaxial cRu-Ni₃N/NF. (e) Ac-STEM image of cRu-Ni₃N. (f) Charge density difference in the cRu-Ni₃N model; (g) DOS of the cRu-Ni₃N and cRu structures. DFT calculations of Ni₃N, cRu, and cRu-Ni₃N models for (h) HER and (i) OER. (j) Schematic for the integrated solar-to-hydrogen system in seawater.

(b, c) Reproduced with permission from ref. [61]. Copyright (2019), Royal Society of Chemistry. (j) Reproduced with permission from ref. [62]. Copyright (2021), Wiley-VCH.

formed by 40 ALD cycles is the most effective in seawater electrolysis. The electrolyzer with NCMS/NiO as both the anode and cathode needs a low voltage of 1.505 V to attain a current density of 100 mA cm⁻² with no apparent decline for over 30 days under industrial conditions.

3.3. Doping regulation

Doping is one of the common strategies to optimize the properties of catalysts. By reasonably introducing one or more metallic or non-metallic elements into the lattice of materials, the electronic

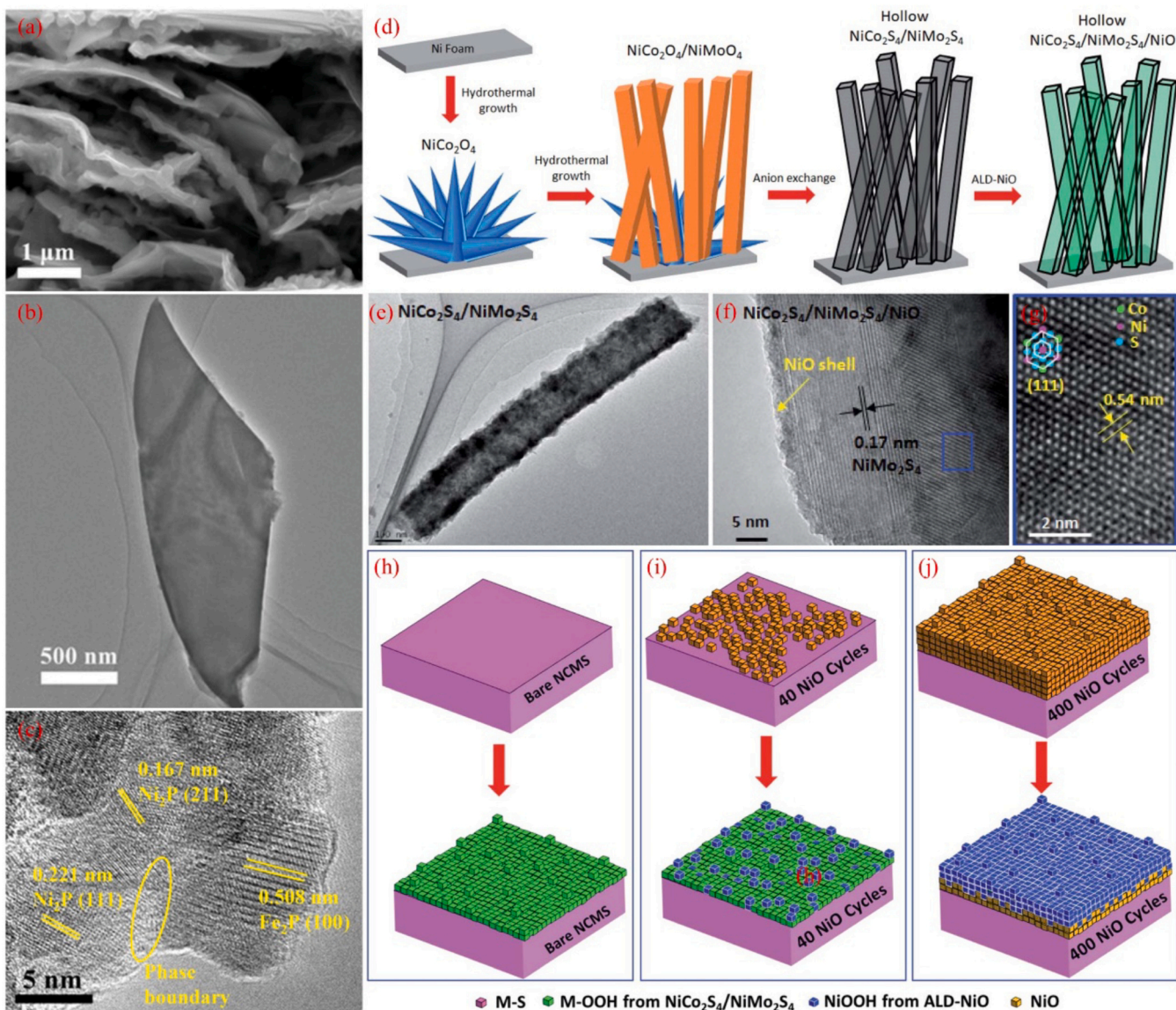


Fig. 6. (a) SEM, (b) TEM, and (c) HR-TEM images of Ni₂P-Fe₂P micro-sheets. (d) Schematic illustration of the fabrication of NiCo₂S₄/NiMo₂S₄/NiO. (e) TEM image of the NCMS catalyst. (f, g) HR-TEM images of NCMS/NiO. Surface reconstruction on (h) NCMS, (i) NCMS/NiO (40 cycles), and (j) NCMS/NiO (400 cycles). (c) Reproduced with permission from ref. [66]. Copyright (2020), Wiley-VCH. (j) Reproduced with permission from ref. [67]. Copyright (2021), Royal Society of Chemistry.

structure can be adjusted to improve the catalytic properties [73–92]. Single-element doping and dual-element doping will be discussed in this section.

3.3.1. Single-element doping

The catalytic activity of bimetallic phosphides in seawater electrolysis can be improved by not only constructing hetero-interfaces but also doping. Wang et al. [93] have synthesized a cobalt-doped Fe₂P electrocatalyst (Co-Fe₂P) (loading: 2.0 mg cm⁻²) on Ni foam by a two-step hydrothermal-phosphating process (Fig. 7a). XPS indicates that Co doping modifies the electronic properties of Fe₂P, making the P part negatively charged (Fig. 7c-d) [94] which can attract protons to enhance the HER activity. Simultaneously, the presence of oxygen-containing functional groups (Fig. 7b) improves the hydrophilicity benefiting HER and OER [95]. The electrolyzer with Co-Fe₂P // Co-Fe₂P couple has excellent catalytic properties in overall seawater splitting as demonstrated by an operating voltage of 1.69 V at 100 mA cm⁻², which is lower than that of the RuO₂ // Pt-C (1.97 V).

Single-element doping can be performed in different ways. Kim et al. [96] have synchronously doped single nickel atoms (Ni_{SA}) and

nickel phosphate clusters (Ni_{Pi}) on the matrix of MoS₂ nanosheets (NSs) supported by one-dimensional (1D)-TiO₂ nanorods (NRs) to produce Ni_{SA}-Ni_{Pi}/MoS₂ NSs/TiO₂ NRs (loading: 7.17 mg cm⁻²) by impregnation and thermal treatment (Fig. 7f-h). According to the calculated free energy diagrams (Fig. 7i-k), when Ni_{SA} and Ni_{Pi} co-existed in the MoS₂ NSs matrix, the electronic properties of the product could be effectively modified, which was favorable for electron transfer and thus played a role in promoting the HER and OER reactions. As a result, the as-prepared electrolyzer with Ni_{SA}-Ni_{Pi}/MoS₂ NSs/TiO₂ NRs acting as both the cathodic and anodic electrodes shows a current density of 10 mA cm⁻² at low cell voltages of 1.52 and 1.66 V beside good stability in long-term operation in simulated seawater and natural seawater, which are lower than that of the Pt/C // RuO₂ couple (1.71 and 1.70 V).

Doping with noble metals can tune the electronic structure of catalysts [99–105] and Ru is more economical than other noble metals. Its binding energy to hydrogen is similar to that of Pt rendering it promising in HER [106–108]. Wu et al. [97] have constructed Ru-incorporated amorphous cobalt-based oxide (Ru-CoO_x/NF) electrocatalyst by *in-situ* growth, anneal, and calcination

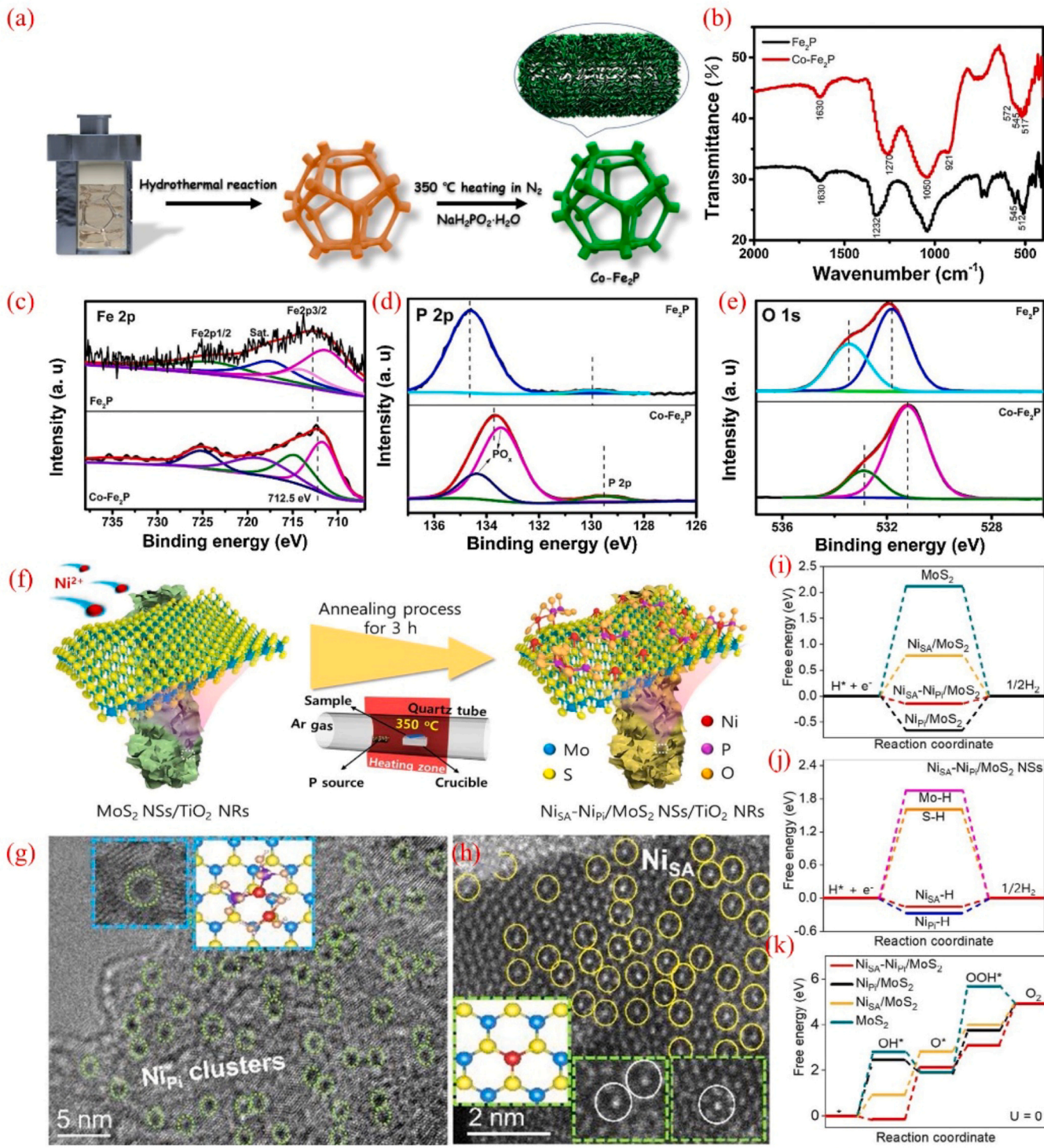


Fig. 7. (a) Schematic for the synthesis process of the Co-Fe₂P electrocatalyst. (b) FT-IR spectra of the Co-Fe₂P electrocatalyst. XPS spectra of (c) Fe 2p, (d) P 2p, and (e) O 1s in the Fe₂P and Co-Fe₂P electrocatalysts. (f) Schematic showing the fabrication of Ni_{SA}-Ni_{Pi}/MoS₂ NSs/TiO₂ NRs. (g) HR-TEM and (h) STEM images of a Ni_{SA}-Ni_{Pi}/MoS₂ nanosheet. (i) ΔG_H of different materials. (j) Comparison of ΔG_H for different sites on Ni_{SA}-Ni_{Pi}/MoS₂. (k) Free energy diagrams of different materials in OER.

(e) Reproduced with permission from ref. [93]. Copyright (2021), Elsevier. (k) Reproduced with permission from ref. [96]. Copyright (2022), Wiley-VCH.

procedure (Fig. 8a). XPS analysis (Fig. 8b-c) indicated that the incorporation of Ru led to charge transfer, which enhanced the electrocatalytic activity. Therefore, the assembled electrolyzer with Ru-CoO_x/NF working as both the anode and cathode electrodes requires low voltages of 2.62 V for a current density of 1 A cm⁻² in seawater electrolysis.

Tran et al. [98] have proposed a catalyst (1D-Cu@Co-CoO/Rh) with continuous Co-CoO containing dispersed Rh atoms and a shell of conductive porous 1D Cu via electrodeposition and electroless deposition step (Fig. 8d). The synergistic effects arising from the uniform Rh atoms and Co-CoO hetero-structures, shown in Fig. 8e, produce rich multi-integrated active sites, optimize the electronic state and lower energy barriers of water dissociation for enhanced

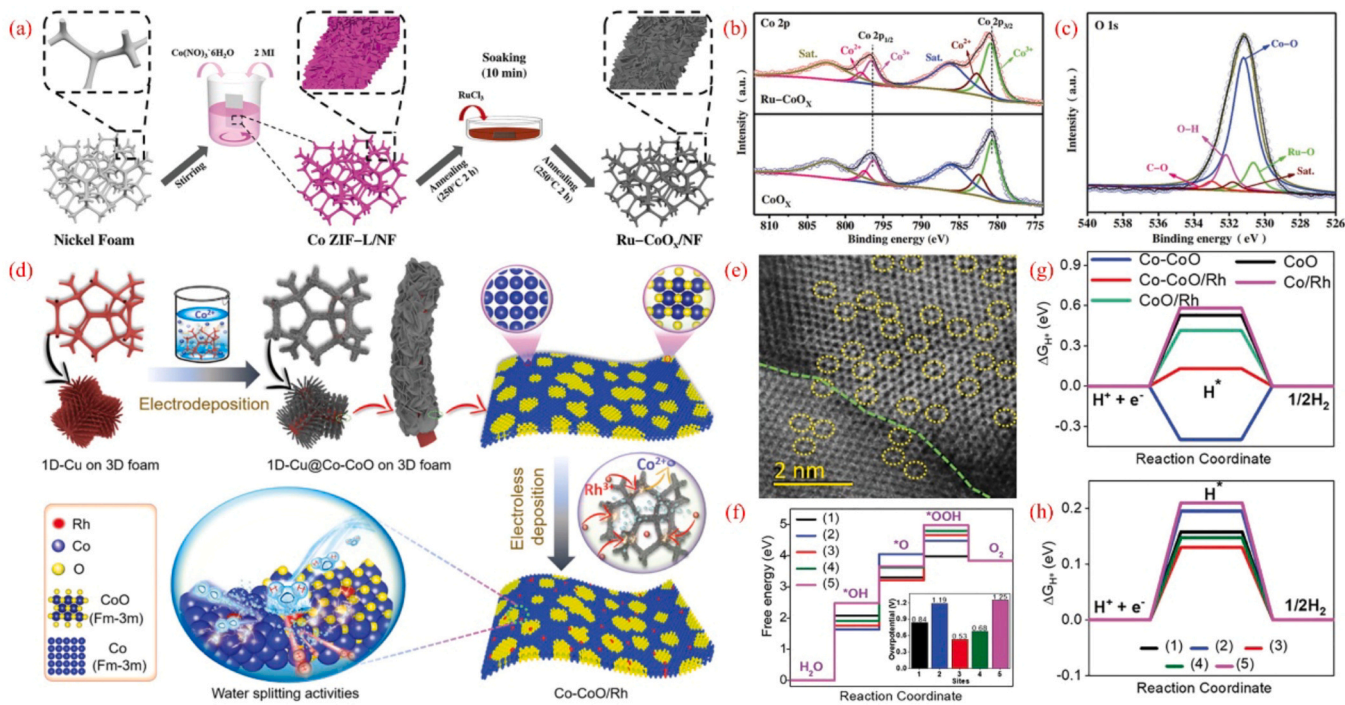


Fig. 8. (a) Schematic illustrating the fabrication of Ru-CoO_x/NF. XPS spectra of (b) Co 2p and (c) O 1s of Ru-CoO_x/NF and CoO_x/NF.(d) Schematic of the preparation of core@shell 1D-Cu@Co-CoO/Rh. (e) STEM image of the Co-CoO/Rh shell. (f) Free energy diagram of OER at different atomic sites on Co-CoO/Rh. (g) ΔG_{H^+} of different materials. (h) ΔG_{H^+} at different atomic sites on Co-CoO/Rh.

(c) Reproduced with permission from ref. [97]. Copyright (2021), Wiley-VCH. (h) Reproduced with permission from ref. [98]. Copyright (2021), Wiley-VCH.

HER and OER activities (Fig. 8f-h). The electrolyzer made with 1D-Cu@Co-CoO/Rh as both the anode and cathode required cell voltages of 1.60, and 1.70 V at 10 mA cm⁻² and robust stability in simulated seawater, and natural seawater, respectively.

3.3.2. Dual-element doping

Multi-element doping exploits the synergistic effects of different heteroatoms and provides the basis to generate more lattice defects, vacancies, and active sites to tailor the catalytic activity [109–115]. In particular, vanadium has an abundant reserve and flexible redox states. V-doped catalysts may be partially disordered structurally because of the partial dissolution of V in the electrolyte to stimulate the reactivity. In OER, V favors the formation of *O and so the activation potential of the catalyst is reduced [116]. Moreover, as the cheapest platinum group metal, Ru is similar to Pt with metal hydrogen bonding strength and abundant d-orbital electrons. It also has a superior ability to adsorb OH⁻ and split water [117]. Consequently, the HER/OER activity of catalysts with an ultra-low amount of Ru introduction can be further promoted without adding excessive cost. Ma et al. [118] have doped RuV-CoNiP/NF catalysts (loading: 3.6 mg cm⁻²) simultaneously with Ru and V by phosphating Ru-impregnated phosphating CoV-LDH on nickel foam (Fig. 9a). The co-doping of Ru with V further facilitated the charge transfer, which was beneficial to accelerating the electrochemical kinetics. In addition, multiple valence states of V existed in the catalyst, which was also more favorable for the redox reaction (Fig. 9b-e). The assembled electrolyzer with RuV-CoNiP/NF as the two electrodes shows 20 mA cm⁻² at only 1.538 V, better than that of the Pt/C/NF // RuO₂/NF (1.678 V), which ranks about the best.

Chang et al. have studied the dual-doping effects by doping with Fe and P on nickel selenide nanoporous films (Fe, P-NiSe₂ NFs) (loading: 1.2 mg cm⁻²) [119]. The electronic structure and surface composition of the Fe, P-NiSe₂ is altered to boost the catalytic activity. According to DFT calculations, Fe doping played a key role in HER, while Ni might be responsible for OER (Fig. 9f-g). Furthermore,

due to the co- incorporation of Fe and P heteroatoms in Fe, P-NiSe₂, its adsorption energy and limiting potential were reduced while its electrical conductivity was increased, all of which boosted the activity, stability, and selectivity of high-efficiency seawater electrolysis (Fig. 9h-j). As a result, a current density of 0.8 A cm⁻² is achieved at 1.8 V for over 200 h in natural seawater feedstock and the properties are better than those of most other electrolyzers and reach the Department of Energy (DOE) 2020 target.(Table 4).

3.4. Others

There are other methods to enhance the activity of seawater splitting electrocatalysts, for instance, *in situ* assembly, alloying, amorphization, and so on. Using the surface etching method, *in situ* assembly of metal oxides/hydroxides can be formed as self-supported electrocatalysts directly on transition metal substrates. Metal corrosion often causes the formation of hierarchical metal oxides or hydroxides which provide easier access to active sites for OER. Moreover, the Mott-Schottky effect may enhance the catalysis between the metal matrix and corrosion layer [120,121] and pre-etching can corrode and remove unstable species from the metal matrix to improve the electrochemical stability. An *in situ* corrosion strategy has been proposed by Duan et al. [122] to construct NiFe hydroxides as free-standing electrodes for overall seawater splitting (Fig. 10a). Owing to the strong interaction between Cl⁻ and metals, HCl was more conducive to the dissolution of Ni than H₂SO₄ and HNO₃, leading to the formation of NiFe hydroxides on the surface of matrixes. *In-situ* Raman spectroscopy confirmed that NiOOH was more likely generated in HCl-c-NiFe rather than H₂SO₄-c-NiFe or HNO₃-c-NiFe (Fig. 10b-e), which played a key role in OER, contributing to enhancing activity for water splitting. In the overall water splitting electrolyzer, HCl-c-NiFe shows low working voltages of 1.62 V at 100 mA cm⁻², which is lower than that of the Pt/C // IrO₂ pair (1.72 V), together with outstanding stability for 300 h in alkaline seawater.

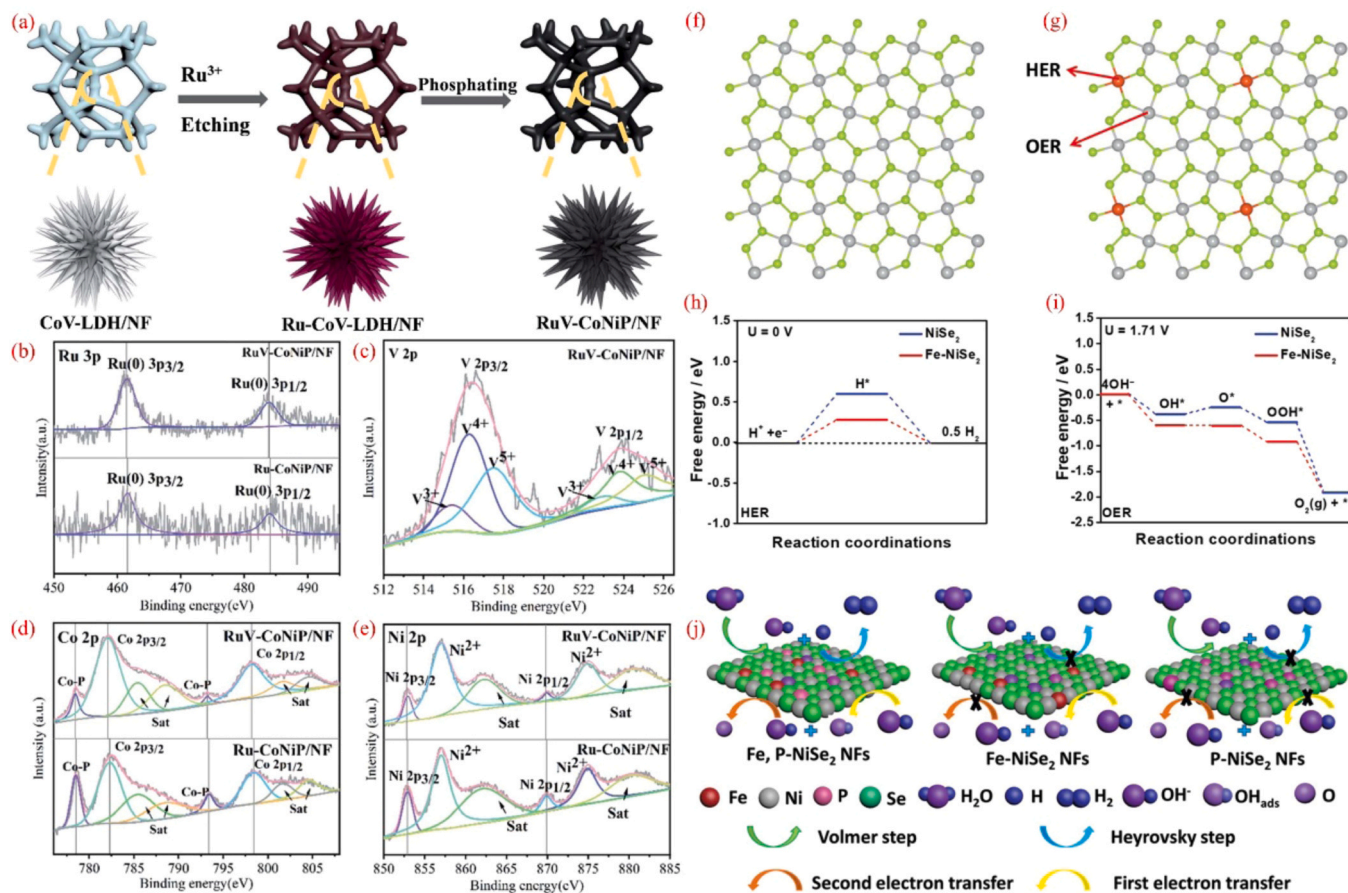


Fig. 9. (a) Schematic illustration of the synthesis for RuV–CoNiP/NF. XPS spectra of (b) Ru 3p, (c) V 2p, (d) Co 2p and (e) Ni 2p in RuV–CoNiP/NF. Surface atomic structures of (f) NiSe₂ and (g) Fe–NiSe₂ with the grey, orange and green balls representing Ni, Fe, and Se atoms, respectively. Simulated free energy diagrams of (h) HER and (i) OER for NiSe₂ and Fe–NiSe₂ at potentials of U = 0 and 1.71 V, respectively. (j) Schematic representation of the HER and OER pathways on different catalysts.

(e) Reproduced with permission from ref. [118]. Copyright (2021), Royal Society of Chemistry. (j) Reproduced with permission from ref. [119]. Copyright (2021), Wiley-VCH.

Table 4

Comparison of recently reported electrocatalysts for overall seawater splitting pertaining to doping regulation.

Electrodes	Voltage (V) @ current density (mA cm ⁻²)	Durability (h)	Electrolytes	Refs.
Co–Fe ₂ P	1.69 @ 100	22	1 M KOH + 0.5 M NaCl	[84]
Ni _{SA} –Ni _{Pt} /MoS ₂ NNs/ TiO ₂ NRs	1.52 @ 10	15	mimic seawater	[87]
1D–Cu@Co–CoO/Rh	1.66 @ 10	15	natural seawater	
Ru–CoO _x /NF	1.60 @ 10	12	mimic seawater	[99]
RuV–CoNiP/NF	1.70 @ 10	12	natural seawater	
RuV–CoNiP/NF	2.62 @ 1000	–	seawater	[98]
Fe, P–NiSe ₂	1.538 @ 20	12	1 M KOH + seawater	[108]
Fe, P–NiSe ₂	1.8 @ 800	200	natural seawater	[109]

Similarly, using a corrosion coordination method, Chen et al. [123] have prepared the 2D–3D nanostructure with metal hydroxides and Prussian blue analogs (PBA) on NiFe foam (Pt–NiFe PBA) by a facile and scalable corrosion approach. The specific morphology produces ample active sites, optimizes the reactions and accelerates mass transport. As a bifunctional electrocatalyst, the Pt–NiFe PBA || Pt–NiFe PBA couple needs 1.48 V to drive 10 mA cm⁻² in 1 M KOH seawater.

In addition to corrosion engineering, *in situ* assembly can be achieved in hydrolysis. Zhang et al. [124] have used the sol–gel method and further annealed to produce the Fe₃O₄/NiC_x composite (NiFe–PBA–gel–cal) (loading: 1.0 mg cm⁻²) that inherits the large specific surface area of the parent structure. *Operando* Raman and XPS analyses indicated that *in-situ* generated FeO and the evolution of Ni(OH)₂ played important roles in HER activity, while *in-situ* generated NiOOH_{2-x} containing high-valence nickel cations and a large number of oxygen defects were mainly responsible for OER

activity (Fig. 10f–l). When integrated electrolyzer with NiFe–PBA–gel–cal as both anode and cathode, a low voltage of 1.66 V is required to provide a current density of 100 mA cm⁻² in simulated seawater and there is no obvious attenuation for 50 h.

Alloying is an effective method to boost the properties of metal catalysts [127,128] by refining the grain size, improving the mechanical strength and specific surface area, and reducing the amounts of single components in order to reduce the cost. The catalytic activity and selectivity can be altered by adding other elements to form alloys to exploit the synergistic effects between components [129,130]. According to the Brewer–Engel valence bond theory [131], alloying metals with unfilled d orbitals and those with internal paired d electrons can enable hydrogen adsorption energy to be tuned on their surfaces to enhance the hydrogen evolution activity. Ros et al. [125] have fabricated an efficient and earth-abundant Ni–Mo–Fe based electrocatalyst by simultaneous electrodeposition on graphitic carbon felts (Fig. 11a). As shown in Fig. 11b–g,

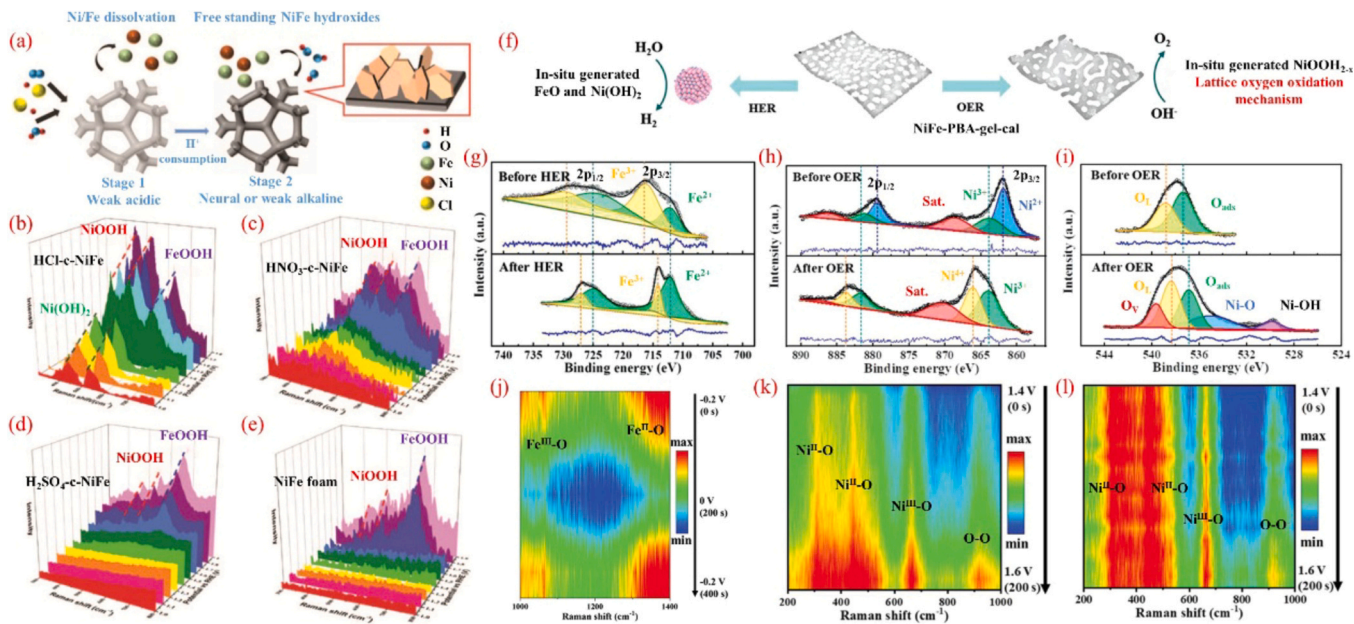


Fig. 10. (a) Synthetic process of HCl-c-NiFe. In situ Raman scattering spectra of (b) HCl-c-NiFe, (c) HNO₃-c-NiFe, (d) H₂SO₄-c-NiFe, and (e) NiFe in the applied potential range between 1.0 V and 1.9 V. (f) Schematic depicting the mechanism of the bifunctional NiFe-PBA-gel-cal catalyst in water hydrolysis. A comparison of XPS spectra at (g) Fe 2p, (h) Ni 2p, and (i) O 1s of NiFe-PBA-gel-cal before and after HER and OER. Operando Raman scattering contour plot of NiFe-PBA-gel-cal with a voltage range from (j) -0.2 to 0 to -0.2 V (vs. RHE) and (k, l) 1.4 to 1.6 V (vs. RHE).

(e) Reproduced with permission from ref. [122]. Copyright (2020), Royal Society of Chemistry. (j) Reproduced with permission from ref. [124]. Copyright (2022), Wiley-VCH.

both the porous thin film and the agglomerated structures were clearly and uniformly composed of Ni-Mo-Fe-O. This trimetallic electrocatalyst exhibited OER performance as good as Ni-Fe and HER

performance as Ni-Mo. Under alkaline conditions, the structure of this Ni-Mo-Fe catalyst undergoes reassembly, leading to enhanced electrocatalytic activity and stability. When assembled electrolyzer

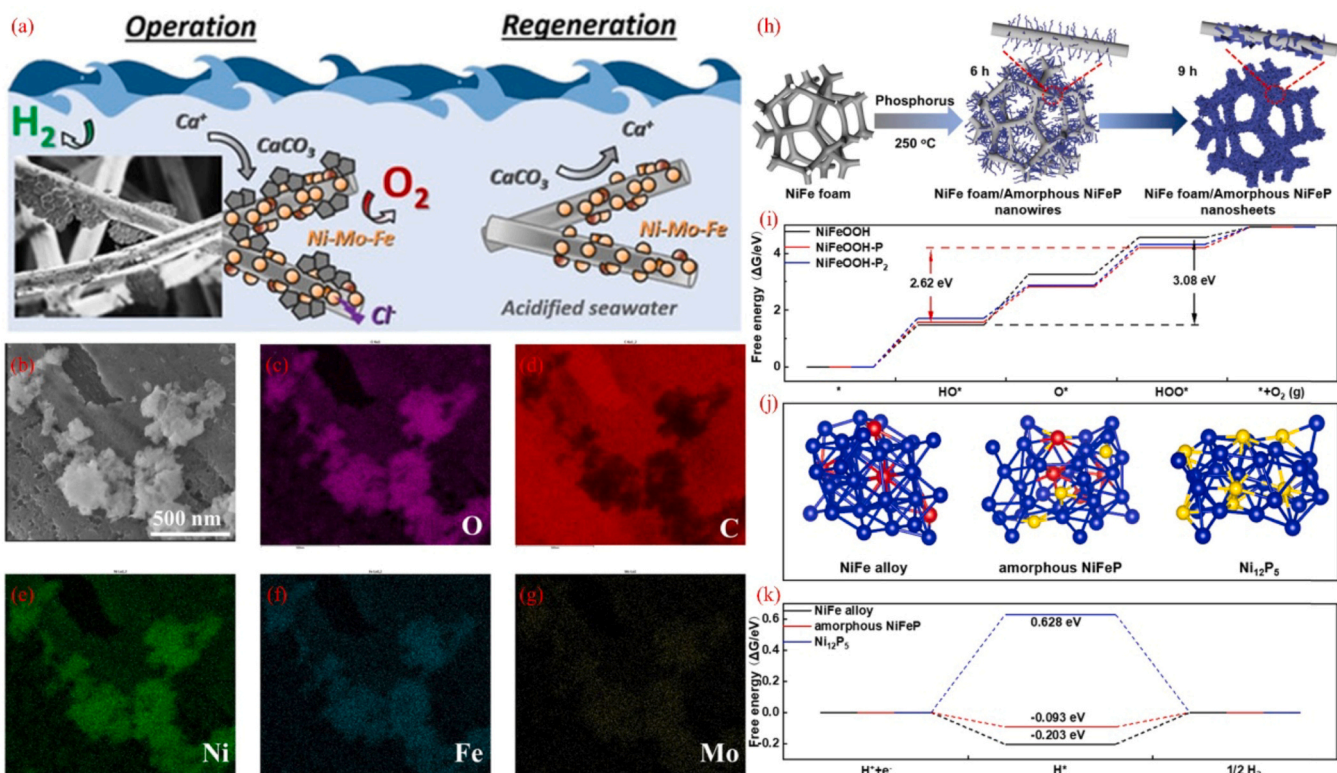


Fig. 11. (a) Schematic illustration of the synthesis of Ni-Mo-Fe. SEM image (b) and corresponding EDS mappings (c–g) of the as-deposited NiMoFe catalyst on graphitic carbon felt. (h) Schematic illustration of the fabrication procedure of NiFeP/NF. (i) Calculated OER results of NiFeOOH, NiFeOOH-P, and NiFeOOH-P₂. (j) Calculated HER models for the NiFe alloy, amorphous NiFeP, and crystalline Ni₁₂P₅. (k) Calculated HER results of the NiFe alloy, amorphous NiFeP, and Ni₁₂P₅.

(c-g) Reproduced with permission from ref. [125]. Copyright (2021), Wiley-VCH. Copyright (2022), Elsevier. (k) Reproduced with permission from ref. [126]. Copyright (2022), Elsevier.

Table 5

Comparison of recently reported electrocatalysts for overall seawater splitting pertaining to other regulations.

Electrodes	Voltage (V) @ current density (mA cm^{-2})	Durability (h)	Electrolytes	Refs.
HCl-c-NiFe	1.62 @ 100	300 12 -	1 M KOH + 0.5 M NaCl 1 M KOH + seawater	[112] [113]
	1.48 @ 10			
	1.56 @ 100			
NiFe-PBA-gel-cal	1.66 @ 100	50 24 500	1 M KOH + 0.5 M NaCl 0.5 M KOH + seawater Simulated alkaline seawater	[114] [120] [132]
	1.59 @ 10			
	1.57 @ 100			
NiMoFe	1.80 @ 1000	-		

with Ni-Mo-Fe || Ni-Mo-Fe couple, it required a low cell voltage of 1.59 V to reach a current density of 10 mA cm^{-2} for more than 24 h stability in 0.5 M KOH seawater, and with an energy efficiency higher than 61.5 %, which had broad application prospects and economic feasibility in seawater electrolysis.

The amorphous structure can improve the catalytic properties by adjusting the arrangement on the atomic scale [132–138]. The short-range atomic arrangement of the amorphous phase increases the density of active centers [139–143] and in seawater electrolysis, the amorphous structure delivers excellent performance. Liu et al. [126] have fabricated amorphous NiFeP/NF electrocatalysts for efficient and stable seawater hydrolysis by a simple and environmentally friendly method (Fig. 11 h). According to the *in-situ* Raman spectra and DFT calculations, the reasons for the excellent catalytic performance of amorphous NiFeP/NF were on the one hand attributed to the reconstruction of the surface structure of NiFeP/NF during the hydrolysis process to continuously exposed new active sites, and on the other hand, the adsorption energy of H^* on metal sites was optimized due to the amorphous structure. The as-prepared electrolyzer with NiFeP/NF employed as both cathodic and anodic electrodes shows current densities of 100 and 1000 mA cm^{-2} at voltages of 1.57 and 1.80 V, respectively. It can be operated for over 500 h in simulated alkaline seawater. (Table 5).

4. Summary and outlook

In this paper, we comprehensively review the principles and challenges of seawater electrolysis and systematically summarize the existing achievements of bifunctional non-noble metal-based electrocatalysts for overall seawater splitting from the perspective of different novel strategies. The following points should be focused on in the future development of electrocatalysts for seawater splitting.

- It is necessary to explore and develop electrocatalysts with high selectivity, activity, and stability to suppress the interference of various cations and chloride ions in natural seawater. Optimization of the electronic structure of catalyst active centers by structure regulation, interfacial regulation, doping regulation, etc., are highly efficient methods to obtain high-performance electrocatalysts for seawater electrolysis [144–146]. Materials with anti-corrosion properties should be selected as the protective layer. Inspired by previous potential candidate materials, artificial intelligence technology can be used as an efficient and convenient tool to screen out qualified electrocatalysts. The large-scale preparation of catalysts with uniform morphology and fine structure also needs to be studied urgently, which is of great significance for the practical application of seawater electrolysis.
- The design of advanced membranes and progressive seawater electrolysis reactors are essential to improve the long-term stability of direct seawater electrolysis processes. The current focus is mainly on the design and synthesis of various catalysts. However, to achieve practical and efficient hydrogen production,

it should be concentrated on the whole reactor not just the catalysts. Besides, seawater splitting should be integrated with interdisciplinary technologies such as advanced membranes, capacitive deionization (CDI) for seawater desalination, and rational design of the seawater electrolysis reactor to achieve the improvement of the overall reaction efficiency through the purification pretreatment.

- A standard platform should be built for the research of direct seawater electrolysis. There are many differences in the composition of seawater around the world, which brings great difficulties to the comparison of different experimental results. The long-term stability test should also specify standardized parameters including uniform service time and current density. Existing catalysts for seawater electrolysis catalysts work well under laboratory conditions with well-defined compositions, concentrations, and pH values. However, these catalysts are still far from excellent performance under industrial and real seawater conditions.
- The clearer mechanism of seawater electrolysis still needs further research. Although the main chlorine-related side reactions have been extensively studied, the inevitable interference and corrosion mechanisms of free metal ions and other halide ions in seawater are still poorly understood. A combination of experimental and computational research could provide a solution to this problem. The use of DFT calculations (including volcano plots, d-band center theory, and adsorption free energy) shows great promise in revealing catalyst reactions and active centers. Novel *in-situ* characterization methods should be developed to track the dynamic structural evolution and active site change of catalysts during practical seawater electrolysis. For example, advanced *in-situ* characterization techniques such as *operando* XAS, Raman, IR, XRD, and TEM are promising to understand the dynamic evolution of catalyst surface active sites, reaction intermediates, and corrosion-resistant layers in real working environments, providing clear principles and guidance for designing efficient catalysts.

In summary, it is highly recommended that more attention should be paid to the material design, device development, standardization of key parameters, and mechanism analysis for electrolysis under real seawater conditions, which will promote the industrialization of seawater electrolysis. This review summarizes the recent progress and perspectives of seawater electrolysis and serves as a reference and guide to foster the rational design of highly efficient catalytic materials for practical seawater splitting. We believe that the realization of large-scale seawater electrolysis for hydrogen production will be industrialized in the near future.

Data Availability

Data will be made available on request.

Declaration of Competing Interest

The authors declare that they have no known competing financial interests or personal relationships that could have appeared to influence the work reported in this paper.

Acknowledgements

The work was funded by the National Natural Science Foundation of China (22075211, U2002213, 21601136, 51971157 and 51621003), the Strategic Research Grant (SRG) of City University of Hong Kong (No. 7005505) and Shenzhen-Hong Kong Innovative Collaborative Research and Development Program (SGLH20181109110802117 and CityU 9240014), Guangdong Province Higher Vocational Colleges & Schools Pearl River Scholar Funded Scheme (2016), Guangdong Third Generation Semiconductor Engineering Technology Development Center (2020GCZX007), Science, Technology, and Innovation Commission of Shenzhen Municipality (RCBS20200714114818140), China Postdoctoral Science Foundation (2019M663118), Double First-Class University Plan (C176220100042), and School level scientific research project of Shenzhen Institute of Information Technology (PT2019E002).

References

- [1] H. Schneider Stephen, The greenhouse effect: science and policy, *Science* 243 (1989) 771–781.
- [2] S. Mallapaty, How China could be carbon neutral by mid-century, *Nature* 586 (2020) 482–483.
- [3] M.S. Dresselhaus, I.L. Thomas, Alternative energy technologies, *Nature* 414 (2001) 332–337.
- [4] A. Turner John, Sustainable hydrogen production, *Science* 305 (2004) 972–974.
- [5] E. Skúlason, V. Tripkovic, M.E. Björketun, S. Guðmundsdóttir, G. Karlberg, J. Rossmeisl, T. Bligaard, H. Jónsson, J.K. Nørskov, Modeling the electrochemical hydrogen oxidation and evolution reactions on the basis of density functional theory calculations, *J. Phys. Chem. C* 114 (2010) 18182–18197.
- [6] I.C. Man, H.-Y. Su, F. Calle-Vallejo, H.A. Hansen, J.I. Martínez, N.G. Inoglu, J. Kitchin, T.F. Jaramillo, J.K. Nørskov, J. Rossmeisl, Universality in oxygen evolution electrocatalysis on oxide surfaces, *ChemCatChem* 3 (2011) 1159–1165.
- [7] H. Liu, Y. Liu, M. Li, X. Liu, J. Luo, Transition-metal-based electrocatalysts for hydrazine-assisted hydrogen production, *Mater. Today Adv.* 7 (2020) 100083.
- [8] C. Wang, H. Shang, L. Jin, H. Xu, Y. Du, Advances in hydrogen production from electrocatalytic seawater splitting, *Nanoscale* 13 (2021) 7897–7912.
- [9] Y. Yao, X. Gao, X. Meng, Recent advances on electrocatalytic and photocatalytic seawater splitting for hydrogen evolution, *Int. J. Hydrol. Energy* 46 (2021) 9087–9100.
- [10] J. Wright, A. Colling, Seawater: Its Composition, Properties, and Behaviour [M]. Pergamon Press, in association with the Open University, 1995.
- [11] V.K. Gouda, I.M. Banat, W.T. Riad, S. Mansour, Microbiologically induced corrosion of UNS N04400 in seawater, *Corrosion* 49 (1993) 63–73.
- [12] B.S. Oh, S.-G. Oh, Y.J. Jung, Y.-Y. Hwang, J.-W. Kang, I.S. Kim, Evaluation of a seawater electrolysis process considering formation of free chlorine and perchlorate, *Desalin. Water Treat.* 18 (2010) 245–250.
- [13] F.J. Millero, R. Feistel, D.G. Wright, T.J. McDougall, The composition of standard seawater and the definition of the reference-composition salinity scale, *Deep Sea Res. Part I: Oceanogr. Res. Pap.* 55 (2008) 50–72.
- [14] Y. Zhao, B. Jin, Y. Zheng, H. Jin, Y. Jiao, S.-Z. Qiao, Charge state manipulation of cobalt selenide catalyst for overall seawater electrolysis, *Adv. Energy Mater.* 8 (2018) 1801926.
- [15] X. Lu, J. Pan, E. Lovell, T.H. Tan, Y.H. Ng, R. Amal, A sea-change: manganese doped nickel/nickel oxide electrocatalysts for hydrogen generation from seawater, *Energy Environ. Sci.* 11 (2018) 1898–1910.
- [16] S. Dresp, F. Dionigi, M. Klingenhof, P. Strasser, Direct electrolytic splitting of seawater: opportunities and challenges, *ACS Energy Lett.* 4 (2019) 933–942.
- [17] G. Liu, Y. Xu, T. Yang, L. Jiang, Recent advances in electrocatalysts for seawater splitting, *Nano Mater. Sci.* (2020), <https://doi.org/10.1016/j.namoms.2020.12.003>
- [18] F. Dionigi, T. Reier, Z. Pawolek, M. Gleich, P. Strasser, Design criteria, operating conditions, and nickel–iron hydroxide catalyst materials for selective seawater electrolysis, *ChemSusChem* 9 (2016) 962–972.
- [19] C. Tang, R. Zhang, W. Lu, Z. Wang, D. Liu, S. Hao, G. Du, A.M. Asiri, X. Sun, Energy-saving electrolytic hydrogen generation: Ni₂P nanoarray as a high-performance non-noble-metal electrocatalyst, *Angew. Chem. Int. Ed.* 56 (2017) 842–846.
- [20] H. Li, L. Zhang, L. Li, C. Wu, Y. Huo, Y. Chen, X. Liu, X. Ke, J. Luo, G. Van, Tendeloo, two-in-one solution using insect wings to produce graphene-graphite films for efficient electrocatalysis, *Nano Res.* 12 (2019) 33–39.
- [21] L. Xie, R. Zhang, L. Cui, D. Liu, S. Hao, Y. Ma, G. Du, A.M. Asiri, X. Sun, High-performance electrolytic oxygen evolution in neutral media catalyzed by a cobalt phosphate nanoarray, *Angew. Chem. Int. Ed.* 56 (2017) 1064–1068.
- [22] Y. Qin, B. Wang, Y. Qiu, X. Liu, G. Qi, S. Zhang, A. Han, J. Luo, J. Liu, Multi-shelled hollow layered double hydroxides with enhanced performance for the oxygen evolution reaction, *Chem. Commun.* 57 (2021) 2752–2755.
- [23] Y. Ji, L. Yang, X. Ren, G. Cui, X. Xiong, X. Sun, Nanoporous CoP₃ nanowire array: acid etching preparation and application as a highly active electrocatalyst for the hydrogen evolution reaction in alkaline solution, *ACS Sustain. Chem. Eng.* 6 (2018) 11186–11189.
- [24] X. Liu, H. Yang, J. He, H. Liu, L. Song, L. Li, J. Luo, Highly active, durable ultrathin MoTe₂ layers for the electroreduction of CO₂ to CH₄, *Small* 14 (2018) 1704049.
- [25] C. Tang, N. Cheng, Z. Pu, W. Xing, X. Sun, Nise nanowire film supported on nickel foam: an efficient and stable 3D bifunctional electrode for full water splitting, *Angew. Chem. Int. Ed.* 54 (2015) 9351–9355.
- [26] S. Gao, M. Jin, J. Sun, X. Liu, S. Zhang, H. Li, J. Luo, X. Sun, Coralloid Au enables high-performance Zn–CO₂ battery and self-driven CO production, *J. Mater. Chem. A* 9 (2021) 21024–21031.
- [27] J. Wang, W. Cui, Q. Liu, Z. Xing, A.M. Asiri, X. Sun, Recent progress in cobalt-based heterogeneous catalysts for electrochemical water splitting, *Adv. Mater.* 28 (2016) 215–230.
- [28] M. Yang, J. Sun, Y. Qin, H. Yang, S. Zhang, X. Liu, J. Luo, Hollow CoFe-layered double hydroxide polyhedrons for highly efficient CO₂ Electrolysis, *Sci. China Mater.* 65 (2022) 536–542.
- [29] X. Liu, Z. Chang, L. Luo, T. Xu, X. Lei, J. Liu, X. Sun, Hierarchical Zn_xCo_{3-x}O₄ nanoarrays with high activity for electrocatalytic oxygen evolution, *Chem. Mater.* 26 (2014) 1889–1895.
- [30] Y. Huo, X. Peng, X. Liu, H. Li, J. Luo, High selectivity toward C₂H₄ production over Cu particles supported by butterfly-wing-derived carbon frameworks, *ACS Appl. Mater. Interfaces* 10 (2018) 12618–12625.
- [31] J. Sun, Y. Li, X. Liu, Q. Yang, J. Liu, X. Sun, D.G. Evans, X. Duan, Hierarchical cobalt iron oxide nanoarrays as structured catalysts, *Chem. Commun.* 48 (2012) 3379–3381.
- [32] Z. Zhao, X. Peng, X. Liu, X. Sun, J. Shi, L. Han, G. Li, J. Luo, Efficient and stable electroreduction of CO₂ to CH₄ on CuS nanosheet arrays, *J. Mater. Chem. A* 5 (2017) 20239–20243.
- [33] L. Yang, Z. Liu, S. Zhu, L. Feng, W. Xing, Ni-Based layered double hydroxide catalysts for oxygen evolution reaction, *Mater. Today Phys.* 16 (2021) 100292.
- [34] D. Li, H. Liu, L. Feng, A review on advanced feni-based catalysts for water splitting reaction, *Energy Fuels* 34 (2020) 13491–13522.
- [35] Y. Mi, S. Shen, X. Peng, H. Bao, X. Liu, J. Luo, Selective electroreduction of CO₂ to C₂ products over Cu₃N-Derived Cu nanowires, *ChemElectroChem* 6 (2019) 2393–2397.
- [36] X. Peng, Y. Chen, Y. Mi, L. Zhuo, G. Qi, J. Ren, Y. Qiu, X. Liu, J. Luo, Efficient Electroreduction CO₂ to CO over MnO₂ Nanosheets, *Inorg. Chem.* 58 (2019) 8910–8914.
- [37] G. Qi, Q. Zhao, Q. Liu, D. Fang, X. Liu, Biomass-derived carbon frameworks for oxygen and carbon dioxide electrochemical reduction, *Ionicics* 27 (2021) 3579–3586.
- [38] H. Chen, Y. Zou, J. Li, K. Zhang, Y. Xia, B. Hui, D. Yang, Wood aerogel-derived sandwich-like layered nanoelectrodes for alkaline overall seawater electro-splitting, *Appl. Catal. B: Environ.* 293 (2021) 120215.
- [39] Y. Li, X. Wu, J. Wang, H. Wei, S. Zhang, S. Zhu, Z. Li, S. Wu, H. Jiang, Y. Liang, Sandwich structured Ni₃S₂–MoS₂–Ni₃S₂/Ni foam electrode as a stable bifunctional electrocatalyst for highly sustained overall seawater splitting, *Electrochim. Acta* 390 (2021) 138833.
- [40] A.R. Jadhav, A. Kumar, J. Lee, T. Yang, S. Na, J. Lee, Y. Luo, X. Liu, Y. Hwang, Y. Liu, H. Lee, Stable complete seawater electrolysis by using interfacial chloride ion blocking layer on catalyst surface, *J. Mater. Chem. A* 8 (2020) 24501–24514.
- [41] H. Wang, L. Chen, L. Tan, X. Liu, Y. Wen, W. Hou, T. Zhan, Electrodeposition of NiFe-layered double hydroxide layer on sulfur-modified nickel molybdate nanorods for highly efficient seawater splitting, *J. Colloid Interface Sci.* 613 (2022) 349–358.
- [42] C. Wang, M. Zhu, Z. Cao, P. Zhu, Y. Cao, X. Xu, C. Xu, Z. Yin, Heterogeneous bimetallic sulfides based seawater electrolysis towards stable industrial-level large current density, *Appl. Catal. B: Environ.* 291 (2021) 120071.
- [43] T.U. Haq, M. Pasha, Y. Tong, S.A. Mansour, Y. Haik, Au nanocluster coupling with Gd–CO₂ nanoflakes embedded in reduced TiO₂ nanosheets: seawater electrolysis at low cell voltage with high selectivity and corrosion resistance, *Appl. Catal. B: Environ.* 301 (2022) 120836.
- [44] J. Liang, Q. Liu, A. Alshehri, X. Sun, Recent advances in nanostructured heterogeneous catalysts for N-cycle electrocatalysis, *Nano Res. Energy* (2022), <https://doi.org/10.26599/NRE.2022.9120010>
- [45] S. Guo, S. Zhang, S. Sun, Tuning nanoparticle catalysis for the oxygen reduction reaction, *Angew. Chem. Int. Ed.* 52 (2013) 8526–8544.
- [46] H. Liu, X. Liu, Z. Mao, Z. Zhao, X. Peng, J. Luo, X. Sun, Plasma-activated Co₃(PO₄)₂ nanosheet arrays with Co³⁺-rich surfaces for overall water splitting, *J. Power Sources* 400 (2018) 190–197.
- [47] D. Qi, F. Lv, T. Wei, M. Jin, G. Meng, S. Zhang, Q. Liu, W. Liu, D. Ma, M. Hamdy, J. Luo, X. Liu, High-efficiency electrocatalytic NO reduction to NH₃ by nanoporous VN, *Nano Res. Energy* (2018), <https://doi.org/10.26599/NRE.2022.9120022>.
- [48] Y. Li, L. Zhang, R. Liu, Z. Cao, X. Sun, X. Liu, J. Luo, WO₃@a-Fe₂O₃ heterojunction arrays with improved photoelectrochemical behavior for neutral pH water splitting, *ChemCatChem* 8 (2016) 2765–2770.

- [49] K. Dang, T. Wang, C. Li, J. Zhang, S. Liu, J. Gong, Improved oxygen evolution kinetics and surface states passivation of Ni-Bi Co-catalyst for a hematite photoanode, *Engineering* 3 (2017) 285–289.
- [50] S. Shen, J. He, X. Peng, W. Xi, L. Zhang, D. Xi, L. Wang, X. Liu, J. Luo, Stepped surface-rich copper fiber felt as an efficient electrocatalyst for the CO₂RR to formate, *J. Mater. Chem. A* 6 (2018) 18960–18966.
- [51] Y. Liang, W. Zhang, D. Wu, Q.-Q. Ni, M.Q. Zhang, Interface engineering of carbon-based nanocomposites for advanced electrochemical energy storage, *Adv. Mater. Interfaces* 5 (2018) 1800430.
- [52] Z. Xie, Y. Qiu, S. Gao, J. Sun, H. Cao, S. Zhang, J. Luo, X. Liu, Surface oxidized ag nanofilms towards highly effective CO₂ reduction, *ChemElectroChem* 8 (2021) 3579–3583.
- [53] L. Chang, Z. Sun, Y.H. Hu, 1t phase transition metal dichalcogenides for hydrogen evolution reaction, *Electrochem. Energy Rev.* 4 (2021) 194–218.
- [54] J. Chen, H. Chen, T. Yu, R. Li, Y. Wang, Z. Shao, S. Song, Recent advances in the understanding of the surface reconstruction of oxygen evolution electrocatalysts and materials development, *Electrochem. Energy Rev.* 4 (2021) 566–600.
- [55] S. Wang, L. Zhao, J. Li, X. Tian, X. Wu, L. Feng, High valence state of Ni and Mo Synergism in NiS₂-MoS₂ hetero-nanorods catalyst with layered surface structure for urea electrocatalysis, *J. Energy Chem.* 66 (2022) 483–492.
- [56] X. Wang, S. Liu, H. Zhang, S. Zhang, G. Meng, Q. Liu, Z. Sun, J. Luo, X. Liu, Polycrystalline SnS_x nanofilm enables CO₂ electroreduction to formate with high current density, *Chem. Commun.* (2022), <https://doi.org/10.1039/D2CC01888H>
- [57] N. Jiang, Q. Tang, M. Sheng, B. You, D.-E. Jiang, Y. Sun, Nickel sulfides for electrocatalytic hydrogen evolution under alkaline conditions: a case study of crystalline NiS, NiS₂, and Ni₃S₂ nanoparticles, *Catal. Sci. Technol.* 6 (2016) 1077–1084.
- [58] K. Xu, P. Chen, X. Li, Y. Tong, H. Ding, X. Wu, W. Chu, Z. Peng, C. Wu, Y. Xie, Metallic nickel nitride nanosheets realizing enhanced electrochemical water oxidation, *J. Am. Chem. Soc.* 137 (2015) 4119–4125.
- [59] M.A. Henderson, The interaction of water with solid surfaces: fundamental aspects revisited, *Surf. Sci. Rep.* 46 (2002) 1–308.
- [60] H. Wu, S. Li, X. Lu, C.Y. Toe, H.Y. Chung, Y. Tang, X. Lu, R. Amal, L. Li, Y.H. Ng, Pulsed electrodeposition of Co₃O₄ nanocrystals on one-dimensional zno scaffolds for enhanced electrochemical water oxidation, *ChemPlusChem* 83 (2018) 934–940.
- [61] Y. Zhao, B. Jin, A. Vasileff, Y. Jiao, S.-Z. Qiao, Interfacial nickel nitride/sulfide as a bifunctional electrode for highly efficient overall water/seawater electrolysis, *J. Mater. Chem. A* 7 (2019) 8117–8121.
- [62] J. Zhu, R. Lu, W. Shi, L. Gong, D. Chen, P. Wang, L. Chen, J. Wu, S. Mu, Y. Zhao, Epitaxially grown Ru clusters-nickel nitride heterostructure advances water electrolysis kinetics in alkaline and seawater media, *Energy Environ. Mater.* (2021), <https://doi.org/10.1002/eem2.12318>
- [63] C. Zhu, A.-L. Wang, W. Xiao, D. Chao, X. Zhang, N.H. Tiep, S. Chen, J. Kang, X. Wang, J. Ding, J. Wang, H. Zhang, H.J. Fan, In situ grown epitaxial heterojunction exhibits high-performance electrocatalytic water splitting, *Adv. Mater.* 30 (2018) 1705516.
- [64] X. Gao, X. Liu, W. Zang, H. Dong, Y. Pang, Z. Kou, P. Wang, Z. Pan, S. Wei, S. Mu, J. Wang, Synergizing in-grown Ni₃N/Ni heterostructured core and ultrathin Ni₃N surface shell enables self-adaptive surface reconfiguration and efficient oxygen evolution reaction, *Nano Energy* 78 (2020) 105355.
- [65] L. Gao, C. Tang, J. Liu, L. He, H. Wang, Z. Ke, W. Li, C. Jiang, D. He, L. Cheng, X. Xiao, Oxygen vacancy-induced electron density tuning of Fe₃O₄ for enhanced oxygen evolution catalysis, *Energy Environ. Mater.* 4 (2021) 392–398.
- [66] L. Wu, L. Yu, F. Zhang, B. McElhenney, D. Luo, A. Karim, S. Chen, Z. Ren, Heterogeneous bimetallic phosphide Ni₂P-Fe₂P as an efficient bifunctional catalyst for water/seawater splitting, *Adv. Funct. Mater.* 31 (2021) 2006484.
- [67] S. Seenivasan, D.-H. Kim, Engineering the surface anatomy of an industrially durable NiCo₂s₄/NiMo₂s₄/nio bifunctional electrode for alkaline seawater electrolysis, *J. Mater. Chem. A* 10 (2022) 9547–9564.
- [68] Y. Li, H. Zhang, M. Jiang, Q. Zhang, P. He, X. Sun, 3D self-supPorted Fe-Doped Ni₂P nanosheet arrays as bifunctional catalysts for overall water splitting, *Adv. Funct. Mater.* 27 (2017) 1702513.
- [69] F. Yu, H. Zhou, Y. Huang, J. Sun, F. Qin, J. Bao, W.A. Goddard, S. Chen, Z. Ren, High-performance bifunctional porous non-noble metal phosphide catalyst for overall water splitting, *Nat. Commun.* 9 (2018) 2551.
- [70] L. Yu, J. Zhang, Y. Dang, J. He, Z. Tobin, P. Kerns, Y. Dou, Y. Jiang, Y. He, S.L. Suib, In situ growth of Ni₂P-Cu₂P bimetallic phosphide with bicontinuous structure on self-supported nicus substrate as an efficient hydrogen evolution reaction electrocatalyst, *ACS Catal.* 9 (2019) 6919–6928.
- [71] H. Zhang, W. Zhou, J. Dong, X.F. Lu, X.W. Lou, Intramolecular electronic coupling in porous iron cobalt (Oxy)phosphide nanoboxes enhances the electrocatalytic activity for oxygen evolution, *Energy Environ. Sci.* 12 (2019) 3348–3355.
- [72] H. Liang, A.N. Gandi, D.H. Anjum, X. Wang, U. Schwingenschlögl, H.N. Alshareef, Plasma-assisted synthesis of nicop for efficient overall water splitting, *Nano Lett.* 16 (2016) 7718–7725.
- [73] H. Lin, N. Liu, Z. Shi, Y. Guo, Y. Tang, Q. Gao, Cobalt-doping in molybdenum-carbide nanowires toward efficient electrocatalytic hydrogen evolution, *Adv. Funct. Mater.* 26 (2016) 5590–5598.
- [74] X. Liu, W. Xi, C. Li, X. Li, J. Shi, Y. Shen, J. He, L. Zhang, L. Xie, X. Sun, P. Wang, J. Luo, L.-M. Liu, Y. Ding, Nanoporous Zn-Doped Co₃O₄ sheets with single-unit-cell-wide lateral surfaces for efficient oxygen evolution and water splitting, *Nano Energy* 44 (2018) 371–377.
- [75] C. Tang, R. Zhang, W. Lu, L. He, X. Jiang, A.M. Asiri, X. Sun, Fe-doped CoP nanoarray: a monolithic multifunctional catalyst for highly efficient hydrogen generation, *Adv. Mater.* 29 (2017) 1602441.
- [76] C. Zhang, H. Liu, Y. Liu, X. Liu, Y. Mi, R. Guo, J. Sun, H. Bao, J. He, Y. Qiu, J. Ren, X. Yang, J. Luo, G. Hu, Rh₂S₃/N-doped carbon hybrids as pH-universal bifunctional electrocatalysts for energy-saving hydrogen evolution, *Small Methods* 4 (2020) 2000208.
- [77] X. Zhang, X. Zhang, H. Xu, Z. Wu, H. Wang, Y. Liang, Iron-doped cobalt monophosphide nanosheet/carbon nanotube hybrids as active and stable electrocatalysts for water splitting, *Adv. Funct. Mater.* 27 (2017) 1606635.
- [78] M. Jin, W. Liu, J. Sun, X. Wang, S. Zhang, J. Luo, X. Liu, Highly dispersed ag clusters for active and stable hydrogen peroxide production, *Nano Res.* (2022), <https://doi.org/10.1007/s12274-022-4208-7>
- [79] T. Liu, D. Liu, F. Qu, D. Wang, L. Zhang, R. Ge, S. Hao, Y. Ma, G. Du, A.M. Asiri, L. Chen, X. Sun, Enhanced electrocatalysis for energy-efficient hydrogen production over CoP catalyst with nonelectroactive Zn as a promoter, *Adv. Energy Mater.* 7 (2017) 1700020.
- [80] H. Liu, X. Peng, X. Liu, G. Qi, J. Luo, Porous Mn-doped FeP/Co₃(PO₄)₂ nanosheets as efficient electrocatalysts for overall water splitting in a wide pH range, *ChemSusChem* 12 (2019) 1334–1341.
- [81] Y. Pan, Y. Liu, Y. Lin, C. Liu, Metal doping effect of the M-Co₂P/nitrogen-doped carbon nanotubes (M = Fe, Ni, Cu) hydrogen evolution hybrid catalysts, *ACS Appl. Mater. Interfaces* 8 (2016) 13890–13901.
- [82] X. Peng, J. Hou, Y. Mi, J. Sun, G. Qi, Y. Qin, S. Zhang, Y. Qiu, J. Luo, X. Liu, Bifunctional single-atomic Mn Sites for energy-efficient hydrogen production, *Nanoscale* 13 (2021) 4767–4773.
- [83] G. Meng, T. Wei, W. Liu, W. Li, S. Zhang, W. Liu, Q. Liu, H. Bao, J. Luo, X. Liu, NiFe layered double hydroxide nanosheets array for high-efficiency electrocatalytic reduction of nitric oxide to ammonia, *Chem. Commun.* (2022), <https://doi.org/10.1039/D2CC02463B>
- [84] H. Liu, X. Peng, X. Liu, Single-atom catalysts for the hydrogen evolution reaction, *ChemElectroChem* 5 (2018) 2963–2974.
- [85] T. Liu, X. Ma, D. Liu, S. Hao, G. Du, Y. Ma, A.M. Asiri, X. Sun, L. Chen, Mn doping of CoP nanosheets array: an efficient electrocatalyst for hydrogen evolution reaction with enhanced activity at all Ph values, *ACS Catal.* 7 (2017) 98–102.
- [86] L. Wang, X. Duan, X. Liu, J. Gu, R. Si, Y. Qiu, Y. Qiu, D. Shi, F. Chen, X. Sun, J. Lin, J. Sun, Atomically dispersed mo supported on metallic Co₉S₈ Nanoflakes as an Advanced Noble-Metal-Free Bifunctional Water Splitting Catalyst Working in Universal ph conditions, *Adv. Energy Mater.* 10 (2020) 1903137.
- [87] L. Wang, G. Qi, X. Liu, Sulfur dopant-enhanced neutral hydrogen evolution performance in MoO₃ nanosheets, *Nanotechnology* 33 (2021) 065701.
- [88] W. Huang, D. Zhou, G. Qi, X. Liu, Fe-doped MoS₂ nanosheets array for high-current-density seawater electrolysis, *Nanotechnology* 32 (2021) 415403.
- [89] H. Liang, H. Zhang, Y. Zong, H. Xu, J. Luo, X. Liu, J. Xu, Studies of Ni-Mg catalyst for stable high efficiency hydrogen storage, *J. Alloy. Compd.* 905 (2022) 164279.
- [90] B. Zhu, L. Fan, N. Mushtaq, R. Raza, M. Sajid, Y. Wu, W. Lin, J.-S. Kim, P.D. Lund, S. Yun, Semiconductor electrochemistry for clean energy conversion and storage, *Electrochim. Energy Rev.* 4 (2021) 757–792.
- [91] S.A. Khalate, S.A. Kadam, Y.-R. Ma, S.S. Pujari, U.M. Patil, Cobalt doped iron phosphate thin film: an effective catalyst for electrochemical water splitting, *J. Alloy. Compd.* 885 (2021) 160914.
- [92] J. Hou, X. Peng, J. Sun, S. Zhang, Q. Liu, X. Wang, J. Luo, X. Liu, Accelerating hydrazine-assisted hydrogen production kinetics with mn dopant modulated Co₂ nanowire arrays, *Inorg. Chem. Front.* 9 (2022) 3047–3058.
- [93] S. Wang, P. Yang, X. Sun, H. Xing, J. Hu, P. Chen, Z. Cui, W. Zhu, Z. Ma, Synthesis of 3D heterostructure Co-Doped Fe₂P electrocatalyst for overall seawater electrolysis, *Appl. Catal. B: Environ.* 297 (2021) 120386.
- [94] R. Boppella, W. Yang, J. Tan, H.-C. Kwon, J. Park, J. Moon, Black phosphorus supported Ni₃P Co-catalyst on graphitic carbon nitride enabling simultaneous boosting charge separation and surface reaction, *Appl. Catal. B: Environ.* 242 (2019) 422–430.
- [95] J. Cai, Y. Song, Y. Zang, S. Niu, Y. Wu, Y. Xie, X. Zheng, Y. Liu, Y. Lin, X. Liu, G. Wang, Y. Qian, N-induced lattice contraction generally boosts the hydrogen evolution catalysis of P-Rich metal phosphides, *Sci. Adv.* 6 (2020) eaaw8113.
- [96] M.S. Kim, D.T. Tran, T.H. Nguyen, V.A. Dinh, N.H. Kim, J.H. Lee, Ni single atoms and Ni phosphate clusters synergistically triggered surface-functionalized MoS₂ nanosheets for high-performance freshwater and seawater electrolysis, *Energy Environ. Mater.* (2022), <https://doi.org/10.1002/eem2.12366>
- [97] D. Wu, D. Chen, J. Zhu, S. Mu, Ultralow Ru incorporated amorphous cobalt-based oxides for high-current-density overall water splitting in alkaline and seawater media, *Small* 17 (2021) 2102777.
- [98] P.K.L. Tran, D.T. Tran, D. Malhotra, S. Prabhakaran, D.H. Kim, N.H. Kim, J.H. Lee, Highly effective freshwater and seawater electrolysis enabled by atomic Rh-modulated Co-CoO lateral heterostructures, *Small* 17 (2021) 2103826.
- [99] L. Zhang, L. Han, H. Liu, X. Liu, J. Luo, Potential-cycling synthesis of single platinum atoms for efficient hydrogen evolution in neutral media, *Angew. Chem. Int. Ed.* 56 (2017) 13694–13698.
- [100] J. Xu, C. Zhang, H. Liu, J. Sun, R. Xie, Y. Qiu, F. Lü, Y. Liu, L. Zhuo, X. Liu, J. Luo, Amorphous MoO_x-stabilized single platinum atoms with ultrahigh mass activity for acidic hydrogen evolution, *Nano Energy* 70 (2020) 104529.
- [101] X. Peng, S. Zhao, Y. Mi, L. Han, X. Liu, D. Qi, J. Sun, Y. Liu, H. Bao, L. Zhuo, H.L. Xin, J. Luo, X. Sun, Trifunctional single-atomic ru sites enable efficient overall water splitting and oxygen reduction in acidic media, *Small* 16 (2020) 2002888.
- [102] X. Peng, Y. Mi, X. Liu, J. Sun, Y. Qiu, S. Zhang, X. Ke, X. Wang, J. Luo, Self-driven dual hydrogen production system based on a bifunctional single-atomic rh catalyst, *J. Mater. Chem. A* 10 (2022) 6134–6145.
- [103] X. Peng, H. Bao, J. Sun, Z. Mao, Y. Qiu, Z. Mo, L. Zhuo, S. Zhang, J. Luo, X. Liu, Heteroatom coordination induces electric field polarization of single Pt sites to promote hydrogen evolution activity, *Nanoscale* 13 (2021) 7134–7139.

- [104] D. Qi, S. Liu, H. Chen, S. Lai, Y. Qin, Y. Qiu, S. Dai, S. Zhang, J. Luo, X. Liu, Rh nanoparticle functionalized heteroatom-doped hollow carbon spheres for efficient electrocatalytic hydrogen evolution, *Mater. Chem. Front.* 5 (2021) 3125–3131.
- [105] X. Liu, J. Liu, Y. Li, Y. Li, X. Sun, Au/Ni₂O₃ arrays with high activity for water oxidation, *ChemCatChem* 6 (2014) 2501–2506.
- [106] Y. Liu, X. Li, Q. Zhang, W. Li, Y. Xie, H. Liu, L. Shang, Z. Liu, Z. Chen, L. Gu, Z. Tang, T. Zhang, S. Lu, A general route to prepare low-ruthenium-content bimetallic electrocatalysts for pH-universal hydrogen evolution reaction by using carbon quantum dots, *Angew. Chem. Int. Ed.* 59 (2020) 1718–1726.
- [107] H. Song, Y. Cheng, B. Li, Y. Fan, B. Liu, Z. Tang, S. Lu, Carbon dots and RuP₂ nanohybrid as an efficient bifunctional catalyst for electrochemical hydrogen evolution reaction and hydrolysis of ammonia borane, *ACS Sustain. Chem. Eng.* 8 (2020) 3995–4002.
- [108] K. Yang, P. Xu, Z. Lin, Y. Yang, P. Jiang, C. Wang, S. Liu, S. Gong, L. Hu, Q. Chen, Ultrasmall Ru/Cu-Doped RuO₂ complex embedded in amorphous carbon skeletoon as highly active bifunctional electrocatalysts for overall water splitting, *Small* 14 (2018) 1803009.
- [109] J. Xu, S. Lai, D. Qi, M. Hu, X. Peng, Y. Liu, W. Liu, G. Hu, H. Xu, F. Li, C. Li, J. He, L. Zhuo, J. Sun, Y. Qiu, S. Zhang, J. Luo, X. Liu, Atomic Fe-Zn dual-metal sites for high-efficiency Ph-universal oxygen reduction catalysis, *Nano Res.* 14 (2021) 1374–1381.
- [110] M. Yang, Y. Liu, J. Sun, S. Zhang, X. Liu, J. Luo, Integration of partially phosphatized bimetal centers into trifunctional catalyst for high-performance hydrogen production and flexible Zn-Air battery, *Sci. China Mater.* 65 (2022) 1176–1186.
- [111] H. Li, W. Wan, X. Liu, H. Liu, S. Shen, F. Lv, J. Luo, Poplar-catkin-derived N, P Codoped carbon microtubes as efficient oxygen electrocatalysts for Zn-Air batteries, *ChemElectroChem* 5 (2018) 1113–1119.
- [112] W. Huang, D. Zhou, H. Yang, X. Liu, J. Luo, Dual-doping promotes the carbon dioxide electroreduction activity of MoS₂ nanosheet array, *ACS Appl. Energy Mater.* 4 (2021) 7492–7496.
- [113] D. Qi, Y. Liu, M. Hu, X. Peng, Y. Qiu, S. Zhang, W. Liu, H. Li, G. Hu, L. Zhuo, Y. Qin, J. He, G. Qi, J. Sun, J. Luo, X. Liu, Engineering atomic sites via adjacent dual-metal sub-nanoclusters for efficient oxygen reduction reaction and Zn-air battery, *Small* 16 (2020) 2004855.
- [114] S. Liu, M. Jin, J. Sun, Y. Qin, S. Gao, Y. Chen, S. Zhang, J. Luo, X. Liu, Coordination environment engineering to boost electrocatalytic CO₂ reduction performance by introducing boron into single-Fe-atomic catalyst, *Chem. Eng. J.* 437 (2022) 135294.
- [115] L. Han, P. Ou, W. Liu, X. Wang, H.-T. Wang, R. Zhang, C.-W. Pao, X. Liu, W.-F. Pong, J. Song, Z. Zhuang, V. Mirkin Michael, J. Luo, L. Xin Huolin, Design of Ru-Ni diatomic sites for efficient alkaline hydrogen oxidation, *Sci. Adv.* 8 (2022) eabm3779.
- [116] T. Zhao, X. Shen, Y. Wang, R.K. Hocking, Y. Li, C. Rong, K. Dastafkan, Z. Su, C. Zhao, In situ reconstruction of V-Doped Ni₂P pre-catalysts with tunable electronic structures for water oxidation, *Adv. Funct. Mater.* 31 (2021) 2100614.
- [117] J. Yu, Q. He, G. Yang, W. Zhou, Z. Shao, M. Ni, Recent advances and prospective in ruthenium-based materials for electrochemical water splitting, *ACS Catal.* 9 (2019) 9973–10011.
- [118] Q. Ma, H. Jin, F. Xia, H. Xu, J. Zhu, R. Qin, H. Bai, B. Shuai, W. Huang, D. Chen, Z. Li, J. Wu, J. Yu, S. Mu, Ultralow Ru-assisted and vanadium-doped flower-like CoP/Ni₂P heterostructure for efficient water splitting in alkali and seawater, *J. Mater. Chem. A* 9 (2021) 26852–26860.
- [119] J. Chang, G. Wang, Z. Yang, B. Li, Q. Wang, R. Kulieev, N. Orlovskaya, M. Gu, Y. Du, G. Wang, Y. Yang, Dual-doping and synergism toward high-performance seawater electrolysis, *Adv. Mater.* 33 (2021) 2101425.
- [120] J. Hou, Y. Sun, Y. Wu, S. Cao, L. Sun, Promoting active sites in core–shell nanowire array as mott-schottky electrocatalysts for efficient and stable overall water splitting, *Adv. Funct. Mater.* 28 (2018) 1704447.
- [121] Z.-H. Xue, H. Su, Q.-Y. Yu, B. Zhang, H.-H. Wang, X.-H. Li, J.-S. Chen, Janus Co/CoP nanoparticles as efficient mott-schottky electrocatalysts for overall water splitting in wide pH range, *Adv. Energy Mater.* 7 (2017) 1602355.
- [122] S. Duan, Z. Liu, H. Zhuo, T. Wang, J. Liu, L. Wang, J. Liang, J. Han, Y. Huang, Q. Li, Hydrochloric acid corrosion induced bifunctional free-standing nife hydroxide nanosheets towards high-performance alkaline seawater splitting, *Nanoscale* 12 (2020) 21743–21749.
- [123] Z. Chen, D. Liu, Y. Gao, Y. Zhao, W. Xiao, G. Xu, T. Ma, Z. Wu, L. Wang, Corrosive-coordinate engineering to construct 2D–3D nanostructure with trace Pt as efficient bifunctional electrocatalyst for overall water splitting, *Sci. China Mater.* 65 (2022) 1217–1224.
- [124] H. Zhang, S. Geng, M. Ouyang, H. Yadegari, F. Xie, D.J. Riley, A self-reconstructed bifunctional electrocatalyst of pseudo-amorphous nickel carbide @ iron oxide network for seawater splitting, *Adv. Sci.* 9 (2022) 2200146.
- [125] C. Ros, S. Murcia-López, X. Garcia, M. Rosado, J. Arbiol, J. Llorca, J.R. Morante, Facing seawater splitting challenges by regeneration with Ni–Mo–Fe bifunctional electrocatalyst for hydrogen and oxygen evolution, *ChemSusChem* 14 (2021) 2872–2881.
- [126] J. Liu, X. Liu, H. Shi, J. Luo, L. Wang, J. Liang, S. Li, L.-M. Yang, T. Wang, Y. Huang, Q. Li, Breaking the scaling relations of oxygen evolution reaction on amorphous NiFeP nanostructures with enhanced activity for overall seawater splitting, *Appl. Catal. B: Environ.* 302 (2022) 120862.
- [127] W. Wan, X. Liu, H. Li, X. Peng, D. Xi, J. Luo, 3D carbon framework-supported coni nanoparticles as bifunctional oxygen electrocatalyst for rechargeable Zn-air batteries, *Appl. Catal. B: Environ.* 240 (2019) 193–200.
- [128] S. Shen, X. Peng, L. Song, Y. Qiu, C. Li, L. Zhuo, J. He, J. Ren, X. Liu, J. Luo, AuCu alloy nanoparticle embedded cu submicrocone arrays for selective conversion of CO₂ to ethanol, *Small* 15 (2019) 1902229.
- [129] Q. Chang, Y. Xu, S. Zhu, F. Xiao, M. Shao, Pt-Ni nanourchins as electrocatalysts for oxygen reduction reaction, *Front. Energy* 11 (2017) 254–259.
- [130] X. Peng, T.J. Omasta, J.M. Roller, W.E. Mustain, Highly active and durable pd-cu catalysts for oxygen reduction in alkaline exchange membrane fuel cells, *Front. Energy* 11 (2017) 299–309.
- [131] M.M. Jakšić, Electrocatalysis of hydrogen evolution in the light of the brewer–engel theory for bonding in metals and intermetallic phases, *Electrochim. Acta* 29 (1984) 1539–1550.
- [132] R.D.L. Smith, M.S. Prévot, R.D. Fagan, S. Trudel, C.P. Berlinguet, Water oxidation catalysis: electrocatalytic response to metal stoichiometry in amorphous metal oxide films containing iron, cobalt, and nickel, *J. Am. Chem. Soc.* 135 (2013) 11580–11586.
- [133] D.L. Smith Rodney, S. Prévot Mathieu, D. Fagan Randal, Z. Zhang, A. Sedach Pavel, J. Siu Man Kit, S. Trudel, P. Berlinguet Curtis, Photochemical route for accessing amorphous metal oxide materials for water oxidation catalysis, *Science* 340 (2013) 60–63.
- [134] L. Kuai, J. Geng, C. Chen, E. Kan, Y. Liu, Q. Wang, B. Geng, A reliable aerosol-spray-assisted approach to produce and optimize amorphous metal oxide catalysts for electrochemical water splitting, *Angew. Chem. Int. Ed.* 53 (2014) 7547–7551.
- [135] J. Yang, J.J. Xu, Nanoporous amorphous manganese oxide as electrocatalyst for oxygen reduction in alkaline solutions, *Electrochim. Commun.* 5 (2003) 306–311.
- [136] A. Indra, P.W. Menezes, N.R. Sahraie, A. Bergmann, C. Das, M. Tallarida, D. Schmeißer, P. Strasser, M. Driess, Unification of catalytic water oxidation and oxygen reduction reactions: amorphous beat crystalline cobalt iron oxides, *J. Am. Chem. Soc.* 136 (2014) 17530–17536.
- [137] A. Bergmann, E. Martínez-Moreno, D. Teschner, P. Chernev, M. Gliech, J.F. De Araújo, T. Reier, H. Dau, P. Strasser, Reversible amorphization and the catalytically active state of crystalline Co₃O₄ during oxygen evolution, *Nat. Commun.* 6 (2015) 8625.
- [138] Z. Yin, R. He, Y. Zhang, L. Feng, X. Wu, T. Wägberg, G. Hu, Electrochemical deposited amorphous feni hydroxide electrode for oxygen evolution reaction, *J. Energy Chem.* 69 (2022) 585–592.
- [139] T. Weber, J.C. Muijsers, J.W. Niemantsverdriet, Structure of Amorphous MoS₃, *The J. Phys. Chem.* 99 (1995) 9194–9200.
- [140] D. Merki, S. Fierro, H. Vrubel, X. Hu, Amorphous molybdenum sulfide films as catalysts for electrochemical hydrogen production in water, *Chem. Sci.* 2 (2011) 1262–1267.
- [141] J.D. Benck, Z. Chen, L.Y. Kuritzky, A.J. Forman, T.F. Jaramillo, Amorphous molybdenum sulfide catalysts for electrochemical hydrogen production: insights into the origin of their catalytic activity, *ACS Catal.* 2 (2012) 1916–1923.
- [142] L. Meng, L. Li, Recent research progress on operational stability of metal oxide/sulfide photoanodes in photoelectrochemical cells, *Nano Res. Energy* (2022), <https://doi.org/10.26599/NRE.2022.9120020>
- [143] C.G. Morales-Guio, X. Hu, Amorphous molybdenum sulfides as hydrogen evolution catalysts, *Acc. Chem. Res.* 47 (2014) 2671–2681.
- [144] J. Hou, X. Peng, J. Sun, S. Zhang, Q. Liu, X. Wang, J. Luo, X. Liu, Accelerating hydrazine-assisted hydrogen production kinetics with Mn dopant modulated CoS₂ nanowire arrays, *Inorg. Chem. Front.* 9 (2022) 3047–3058.
- [145] G. Meng, T. Wei, W. Liu, w Li, S. Zhang, W. Liu, Q. Liu, H. Bao, J. Luo, X. Liu, NiFe layered double hydroxide nanosheets array for high-efficiency electrocatalytic reduction of nitric oxide to ammonia, *Chem. Commun.* (2022), <https://doi.org/10.1039/D2CC02463B>
- [146] H. Zhang, Y. Qiu, S. Zhang, Q. Liu, J. Luo, X. Liu, Nitrogen-incorporated iron phosphosulfide nanosheets as efficient bifunctional electrocatalysts for energy-saving hydrogen evolution, *Ionics* (2022), <https://doi.org/10.1007/s11581-022-04634-z>